Journal of Archaeological Science: Reports 42 (2022) 103385

Contents lists available at ScienceDirect

Journal of Archaeological Science: Reports

journal homepage: www.elsevier.com/locate/jasrep

Far from flint: Inferring land-use and social networks from Middle and Upper Palaeolithic lithic assemblages (Cardina-Salto do Boi, Côa Valley, Portugal)

Thierry Aubry [a,b,*], António Fernando Barbosa [a], Cristina Gameiro [b], Luís Luís [a,b], André Tomás Santos [a,b], Marcelo Silvestre [a]

[a] Côa Parque, Fundação para a Salvaguarda e Valorização do Vale do Côa, Rua do Museu, 5150-610 Vila Nova de Foz Côa, Portugal
[b] UNIARQ – Centro de Arqueologia Universidade de Lisboa, Faculdade de Letras, Alameda da Universidade, 1600-214 Lisboa, Portugal

ARTICLE INFO

Keywords:
Lithic raw material
Lithic technology
Neanderthal
Anatomically modern human
Iberia

ABSTRACT

Hunter-gatherer societies mobility has been interpreted as a dialectical interplay of social and environmental factors. Demography and social network restriction have been pointed out as potential factors for the demise of Neanderthal and to differ them from anatomically modern human. To reconstruct land use and social network we investigate Middle and Upper Palaeolithic lithic remains from an open-air site located in Iberian hinterland, spanning from MIS 5 to 3. In a geological environment with a variety of quartz veins but no available flint or silcrete sources, data reveal common patterns through Neanderthal occupations, and substantial differences interpreted as distinct subsistence strategies and social networks of the two populations.

1. Introduction

Replacement of Neanderthal by anatomically modern human (AMH) populations (Green et al., 2010; Higham et al, 2014; Hublin et al., 2020) and the interpretation of the archaeological record as cognitive evidence (d'Errico, 2003; Langley et al., 2008) are still hardly debated questions in the study of Prehistory. In the absence of human skeletal remains, bone and stone tool technology have been used to document the first appearance, the east–west dispersal of AMH, and its relation with the last Neanderthal populations (Zilhão, 2006; Hoffecker, 2009; Hublin, 2015; Zilhão et al., 2017; Straus, 2020).

The Upper Palaeolithic record has been considered as different from previous material culture because of the appearance of types of archaeological materials that allow the distinction of geographical groups and the definition of time–space cultures (Gilman, 1984). It has been argued that the sudden emergence of ornaments, figurative art, and the coeval replacement of Neanderthals by AMH, about 40,000 years ago, is not a coincidence (Klein, 2003). This change, named the Upper Palaeolithic revolution (Gilman, 1984; Mellars, 1994; Mellars, 2005; Bar-Yosef, 2002), which began with the Aurignacian in Western Europe, has been characterized by, among other things, (1) a rapid diversification of human artefacts, including a variety of specialized tools and weapons, body ornaments, and (2) the emergence of symbolic thought as evidenced in part by cave drawing.

However, the question of whether archaeological record supports or not this interpretation and the extent to which Neanderthals and AMH behaviours differ has been hardly debated (Zilhão, 2001, Zilhao, 2007; Shea, 2011; Villa and Roebroeks, 2014). For the last 10 years, studies have revealed archaeological evidence that Neanderthal symbolic thinking thus emerged and developed in a gradual manner in different regions of Europe, before the arrival of AMH, on object, cave wall or ground (Peresani et al., 2011; Radovčić et al., 2015; Jaubert et al., 2016; Hoffmann et al., 2018a; Hoffmann et al., 2018b; Martí et al., 2021).

The study of stone tools raw material sources has been used as a proxy of past foragers behaviours using location and distance of transfer (Brantingham, 2006), based on geochemical and geological methods for the characterization of flint microfacies and determination of the geographical location of their sources (Masson, 1981; Demars, 1985; Geneste, 1985; Tarriño, 2001; Mangado Llach, 2005; Fernandes and Raynal, 2006; Delvignes, 2016; Sánchez de la Torre et al., 2017). Lithic raw material sourcing studies can also document changes in resource exploitation strategies through time, reflecting forager economic and seasonal variability (Féblot-Augustins, 1993, 1999). Distances of displacement, raw material quality and quantities present at a specific

* Corresponding author at: Côa Parque, Fundação para a Salvaguarda e Valorização do Vale do Côa, Rua do Museu, 5150-610 Vila Nova de Foz Côa, Portugal.
E-mail address: thierryaubry@arte-coa.pt (T. Aubry).

https://doi.org/10.1016/j.jasrep.2022.103385
Received 15 August 2021; Received in revised form 10 February 2022; Accepted 14 February 2022

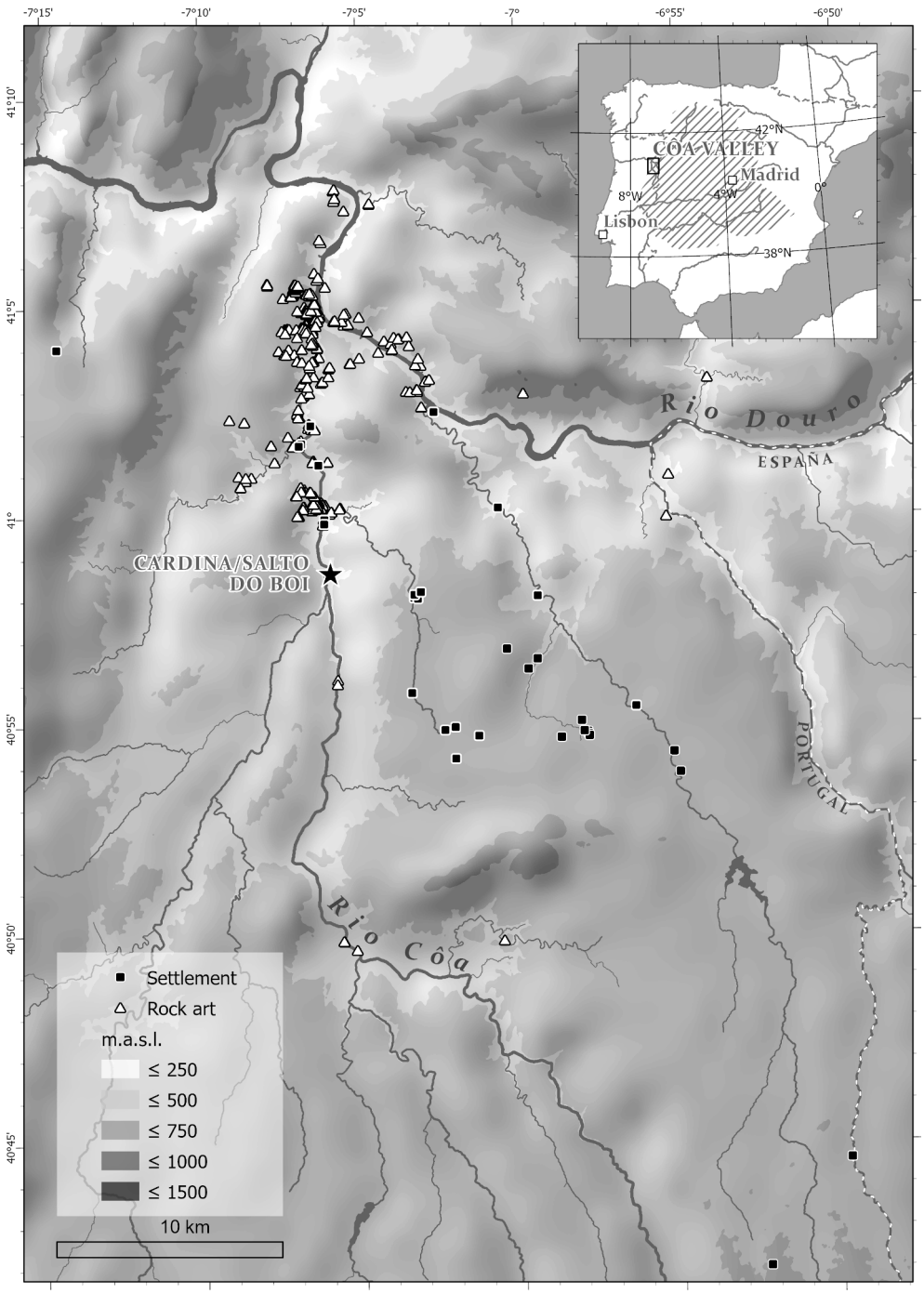

Fig. 1. Location of the Cardina-Salto do Boi site in the Palaeolithic rock art and occupation context of the Côa Valley.

site and the documentation of different lithic reduction phases, leading to artefact abandonment using the *chaîne opératoire* concept (Leroi-Gourhan, 1964; Geneste, 1985, Soressi and Geneste, 2011), are essential to reconstruct past forager's mobility and land-use strategies.

Nevertheless, lithic raw material sources may express non-utilitarian purposes and raw materials of an archaeological assemblage can therefore be the result, not only of direct procurement (Binford, 1980) but also of exchange (Kelly, 1983; Gamble, 1999). This is the case of long-distance raw materials, which have been used to define social networks, fundamental for human survival as the expression of immaterial behaviours, such as information exchange (Whallon, 2006; Burke, 2012).

Within this general framework, AMH behaviours have been differentiated from the Neanderthal based on the low frequency of long-distance lithic raw materials transfer (>100 km) interpreted in terms of land-use strategies and mobility (Féblot-Augustins, 1993, Féblot-Augustins, 1999; Fernandes et al., 2008; Turq et al., 2017). Even though, studies in Western Europe have shown that Neanderthal lithic production can be complex, revealing a cognitive capacity for long-term working memory (Eren and Lycett, 2012), and an extensive knowledge and intensive exploitation of the lithic resources within 50 km, displacement of specific flint from sources exceeding that distance is rare (Geneste, 1988; Féblot-Augustins, 1999; 2009; Fernandes et al., 2008; Delagnes and Rendu, 2011; Turq et al., 2017; Gómez de Soler et al., 2020, Abrunhosa et al., 2020; Prieto et al., 2021).

Studies of the Upper Palaeolithic assemblages from Côa Valley sites,

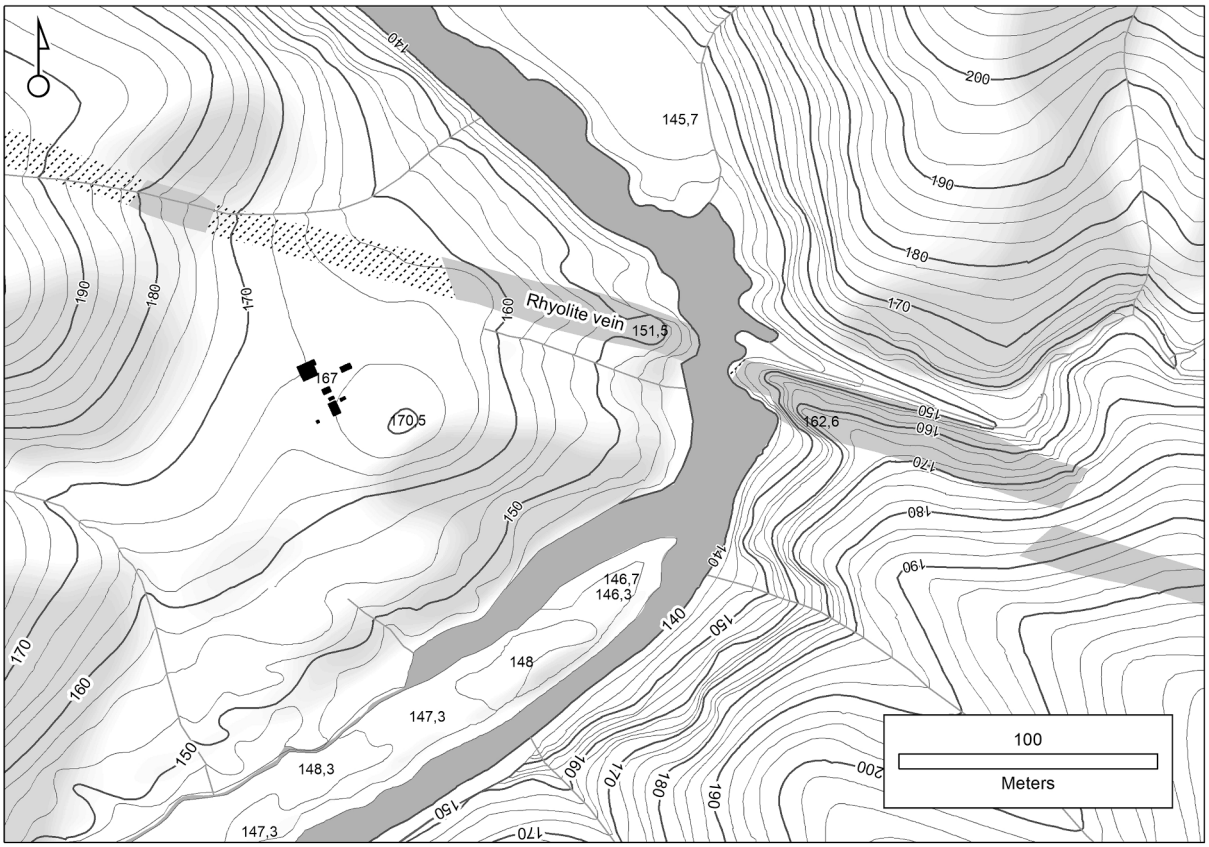

Fig. 2. Topographic map of the Cardina-Salto do Boi site and excavated area at the end of the 2019 field season.

situated in North-eastern Portugal (Fig. 1), have provided evidence of low proportion (<5%) of flint and silcrete from the Lusitanian Basin, the Tagus and Douro Basin in Northern and Southern Meseta, transferred from 100 to 250 km (Mangado Llach, 2005; Aubry et al., 2012, 2016b). We have proposed that Upper Palaeolithic Côa Valley raw material procurement express a three-level model for social interaction, which involves embedded procurement, long-distance raw material exchange, and symbolic community, reflected by the largest concentration of open-air Upper Palaeolithic rock art in Europe (Aubry et al., 2012, Aubry et al., 2016b).

New excavations of the Middle Palaeolithic occupations layers at Cardina-Salto do Boi, one of the Côa Valley sites, provide an opportunity to improve the inference established from 6 m^2 (Aubry et al., 2016a, Aubry et al., 2020) and identify representative patterns of lithic procurement strategies during Middle and Early Upper Palaeolithic, in a region far from flint sources.

2. Cardina-salto do boi site and archaeostratigraphic sequence

The open-air site of Cardina-Salto do Boi, located in the Iberian hinterland (Fig. 1) was the first Upper Palaeolithic site discovered in the Côa Valley, providing evidence of the existence of an archaeological context for the open-air rock art discovered in 1991. This discovery of engraved panels in outcrops distributed in the landscape demonstrated its use for symbolic purposes and changed our understanding of Palaeolithic rock art (Zilhão et al., 1995). The archaeological remains are found on a topographic platform on the left margin of the Côa River, at 167,5 m above sea level, and 20 m above the present-day Côa riverbed (Fig. 2). A rhyolite dike with E/W direction crosses the site and the river in a place locally named Salto do Boi (Ox's Leap).

Between 1995 and 2001 excavation of 12 m^2 in one area of the site (Fig. 3, sector N/O) have revealed a colluvial sequence composed of 5 units. The uppermost metre (layers 4b to 1) is a sequence of slope deposits resulting from gravity-driven processes, accumulating with the concurrent action of water, with some evidence of pedogenesis and anthropogenic inputs and disturbances (Bergadà, 2009). Layers 4b and 4 contain lithic remains of several occupations of the site, from the Final Gravettian to the present-day (Zilhão et al., 1995; Aubry, 2009). The thermoluminescence ages obtained on seven burnt quartzite pebbles recovered at the bottom of the layer 4 range from 20.7 ± 1.3 to 30.1 ± 1.5 ka, with 5 out of 7 clustered in the 26.5–30 ka interval (Valladas et al., 2001) in agreement with the attribution based on the lithic assemblage assigned to the end of the Gravettian (Zilhão et al., 1995).

New excavation realized between 2014 and 2019 in 3 different areas of the site (Fig. 3) have exposed a 3.5 m-thick sequence of alluvial deposits designated as Geoarchaeological Field Units (GFUs): GFU 5 to GFU 8 (Fig. 3, section A, sector H'/I'-17/19). Geological study of these deposits has revealed that they reflect relatively stable floodplain conditions (Dimuccio et al., 2019), and the refitting of lithic remains has shown that the vertical dispersal of the original occupation contexts does not exceed 20 cm (Aubry et al., 2020). In the context of overbank alluvial inundation, the explanation for the scatter lies in the rise of groundwater levels and the rapid decrease of water-flow energy at the end of the sedimentation process (Zilhão, 2021).

The 2015 excavation on 6 m^2 has revealed the existence of discoid (centripetal and unifacial) reduction sequence to the production of flake blanks with a few proportions of notches, denticulates, and sidescrapers, under the UA 11 of GFU 5, that have been attributed to the Middle Palaeolithic, based on technology (Aubry et al., 2016a). Further works in 2017, 2018 and 2019 have provided more technological evidence of the existence of Middle Palaeolithic assemblages in GFU 5, 6 and 7, but also of blades and bladelets reduction sequence in the upper part of the GFU 5 (Aubry et al., 2020).

Eleven luminescence ages were obtained for GFU 5, on feldspar

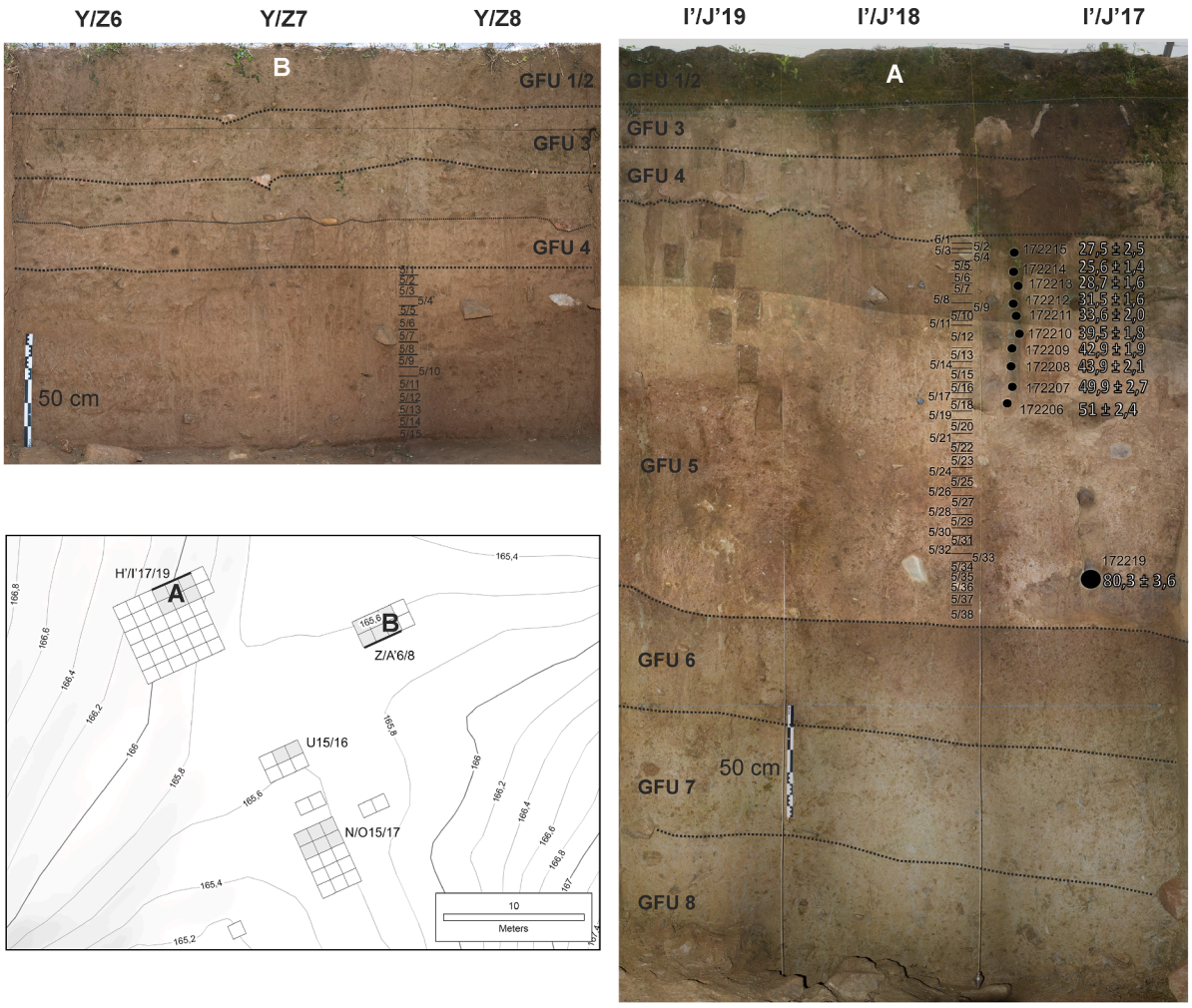

Fig. 3. Stratigraphic sequence, geoarchaeological field unit (GFU), and samples location for Fading-corrected pIRIR(50,225) luminescence ages in the reference cross-section A and B.

grains using a multi-grain two post-IR IR (pIRIR) SAR protocols, whereby the pIRIR signal was measured after IR stimulation at 50 °C and at 225 °C and the final ages were corrected for anomalous fading (Aubry et al., 2020). The ages obtained have confirmed the attribution to the Middle Palaeolithic of the lower part of the GFU 5 and the ages obtained from samples 172,213 to 172,215 (25.6 ± 1.4 to 28.7 ± 1.6 interval), at the top of the GFU 5, are statistically equivalent to the results obtained by thermoluminescence for the base of GFU 4 (26.5 ± 1.8 to 30.1 ± 1.5 ka), from five heated quartzite pebbles found at the bottom of the layer 4, recovered in the squares Q-16/17 near the area N/O (Valladas et al., 2001, Fig. 3).

The ages for sample 172,210 (39.5 ± 1.8) and sample 172,211 (33.6 ± 2.0 ka), along with geological and micromorphological data (Dimuccio et al., 2019) reveal a discontinuity at the Middle/Upper Palaeolithic boundary, which age-depth modelling using Bayesian Statistics constraint to the interval between 34.0 ± 2.0 and 38.4 ± 1.9 ka (Aubry et al., 2020, Fig. 3). The data obtained at Cardina-Sato do Boi have been interpreted as an evidence of an alluvial deposition event in southern Iberia, post-dating 40–42 ka, containing Middle Palaeolithic lithic technology, confirming the late persistence of the Middle Palaeolithic and Neandertals in southern Iberia (Zilhão, 2021).

3. Materials and methods

Lithic remains studied (80,666 pieces including 72,252 knapped pieces) have been recovered in 20 m2 from four test areas of the Cardina-Salto do Boi site (Fig. 2, H'/I'-17/19, Z/A'-6/8, U-15/16, N/O-15/17). The GFUs 4, 5, 6 and 7 have been excavated by 5-cm-thick artificial units (UAs) for the non-piece-plotted recovered by water sieving with 2-mm grids (Fig. 3). Inside each GFU, the 5-cm-thick artificial units were numbered sequentially per, by square-meter unit of the excavation grid. All the fragments larger than 5 cm detected during the excavation of each artificial unit have been drawn and plotted in three dimensions.

The method and database used to detect, characterize, and study siliceous rocks used to produce knapped stone-tool relies on the survey, macroscopic and microscopic analysis on thin section of selected samples. The Cardina-Salto do Boi lithic remains, and geological samples, have been systematically observed with a Leica Stereomicroscope, up to 100x, equipped with software for picture management.

The survey of potential siliceous rocks sources for stone tools from Portugal has been orientated on geological data provided by the Instituto Geológico e Mineiro de Portugal (Carta Geológica de Portugal, Scale 1:50,000) and the inventory of Portuguese mineral occurrences and resources (SIORMINP).

Flint and silcrete have been studied using the facies type analyses of

Table 1
Code convention used to describe fine-grained siliceous rock categories identified in the Côa Valley series and quartz vein categories (Types follow the code convention proposed in Aubry et al., 2012, Expolaire colour code (Cailleux, 1992) and gytological types defined by Fernandes et al., 2008, as follows: 0 (in situ outcrop), 1 (subprimary outcrops), 2 (colluvial gathering), 3 (recent river deposits), 4 (old alluvial deposits), and 5 (only observed in archaeological sample); Ch (undetermined chalcedony), Ch-LF (chalcedony length-fast), cQ (cryptocristalline quartz), cQ-mQ (cryptoquartz/microquartz), MQ (macroquartz), mQ (microquartz), Op (opal), Biv (bivalve), Bryo (Bryozoa), Char-G (Charophytes gyrogonite), Char-S (Charophytesstem), CRI (crinoids), DIA (diatom), ECH (echinoid), SpS-m (monoaxone spicule), SpS-t (triaxone spicule), For (foraminifera), Gas (gastropod), Ins (insertae sedis), Ost (ostracod), Ca (calcite), Mus (muscovite) Of (iron oxide), Q-ter (terrigenous quartz).

Genetic	CA variable	Code	Gytology		Description	Mineralogy/Porosity/ Allochems	Precursor	Environment
Flint/Chert	**CP**	**A1**	0/1/2	Anadia red flint	Translucent to sub-opaque, brechoid or homogeneous structure, dark brown–red red, light red, light brown–red (S29, S20, N30, N15)	mineralogy (cQ, Ch-LF, MQ, Of), moldic (MQ) and tectonic (Ca) porosity, terrigenous quartz (<10%). Sandstone cortex. Bedded and nodular flint	Mesozoic-Early Jurassic - Early Hettangian - Pereiros formation	Marginal marine
		C1a	0/1/2/3/ 4	Sicó Massif grey flint	Opaque, homogeneous or mottled structure, grey, pink-grey, pale brown (N31, M31, M30, L71)	mineralogy (mQ, Ch-LF, Cal-m, Of), tectonic (Ca, Of) porosity, non skeletal coated peloids, skeletal allochems (For-P, SpS, Biv). Fresh cortex <5 mm or white neocortex. Thalassinoïd nodular flint	Mesozoic - Jurassic- Middle/Upper Bajocian - Degracias formation	Base of continental slope
		C3a	0/1/2	Outil/Ançã banded and mottled flint	Sub-opaque to opaque, laminated, Liesegang and multi-Liesegang rings structure, Liesegang struture parallel to the cortex, white, weak red, pink, weak brown, pale brown, red-brown, grey-pink to brown (P70, K92, N11, M30, M53, M13, M71, L69, L71, N13, N55, P70)	mineralogy (cQ-mQ, Ch-LF, Cal-m), moldic and vuggy porosity (MQ), tectonic fracture filled by yellow Of (M65), pelloïdes non skeletal coated grains, skeletal allochems (For, Sps-m, SpS-t, Biv). Fresh to neocortex (<5mm). Thalassinoïd nodular flint	Mesozoic - Jurassic - Middle/Upper Bajocian - Ançã formation	Inner-middle ramp
		C3b	0/1/2/4	Outil/Ançã epigenetic flint	Sub-opaque to sub-translucide, homogeneous and Liesegang structure, white, weak red, pink, weak brown, pale brown, red-brown, grey-pink (K92, N11, M30, M53, M13, M71, L69, L71, N13, N55)	peloïds coated non skeletal grains relict, tectonic fracture filled by yellow Of (M65), skeletal allochems (P-For, Sps-m, SpS-t, Biv, Ins). Fresh to neocortex (<5mm). Thalassinoïd nodular flint	Mesozoic - Jurassic - Middle/Upper Bajocian - Ançã formation	Inner-middle ramp
		D1/ 2	0/1/2/4	Nabão black to grey mottled and speckled flint	Sub-opaque to opaque, black to grey (T92, M30, T31, K31), brechoid and Liesegang rings structure	mineralogy (cQ-mQ (60–80%), mQ(<5%),Ch-LF(5–10%), Of, Ca (15–20%), tectonic (Ch-LF) and moldic bioclast (Ch-LF, MQ) porosity, peloids and pisoids non skeletal coated grains, skeletal allochems (Gas, Char-g, Cha-s, Ost). Fresh to neocortex. Thalassinoïd nodular flint	Mesozoic- Jurassic - Middle/Upper Oxfordian - Cabaços formation	Lacustrine/ marginal marine
		D3	0/1/2/4	Nabão black to grey translucent flint	Sub-opaque to sub-translucide, black to grey (S30, P30, M30, T31-K31), homogeneous and Liesegang rings structure	(cQ-mQ/O), tectonic (Ch-LF) and moldic tectonic (Ch-LF, MQ) porosity, peloids and pisoids non skeletal coated grains, skeletal allochems (Gas, Char-g, Cha-s, Ost). Fresh cortex to neocortex. Thalassinoïd nodular flint	Mesozoic - Jurassic - Middle/Upper Oxfordian - Cabaços formation	Lacustrine/ marginal marine
		E4	0/1/2/4	Caxarias grey/ brown banded and mottled flint	Translucent to sub-opaque, light grey, pink-grey, grey, pink, light brown–red, grey, grey red (L31, M29, M30, M31, M70, N30, N71, P53), Liesegang rings structure parallel to the cortex, mottled red (Of) and grey circular (burrow?, 1–5 mm, mQ)	(cQ, MQ, Op), moldic bioclasts (MQ, Ch-LF) porosity, non skeletal allochems (Q-ter, Mus, Of), peloids relict non skeletal coated allochems, skeletal allochems (For, SpS). Fresh cortex (>5mm) and neocortex grey (N71) and sub-cortical white to grey (M70), infra-cortex Of	Mesozoic - Cretaceous - Upper Cenomanian - Carbonate body	Inner platform rudists buildups

(*continued on next page*)

Table 1 (*continued*)

Genetic	CA variable	Code	Gytology		Description	Mineralogy/Porosity/ Allochems	Precursor	Environment
						line. Thalassinoïd nodular flint		
		E1	0/1/2/4	Limestone and Montejunto massif red flint	Translucent to sub-opaque, red, brown to yellow (S15, R25, S19, P27, N27, T30, M30, L60), epigenetic laminated or Liesegang rings structures parallel to the cortex	(cQ, mQ (90%), OF), geodes (MQ), moldic/ fenestral (MQ, Ch-LF) porosity, peloïd relicts, skeletal grains (bryo, Biv, For, SpS). Neocortex <5 mm. Thalassinoïd nodular flint	Mesozoic - Cretaceous - Upper Cenomanian - Carbonate body	Inner platform rudists buildups
Silcrete	**DB**	**I1**	0/1/2/4	Indiferenciated azoïc sub-translucent light grey to bluish silcrete			Cenozoic - Neogene	Continental, lacustrine/ groundwater
		I11	0/1/2/3/ 4	Diagenetic sub-translucent light grey to bluish silcrete			Cenozoic - Neogene	Continental, lacustrine
		I2a	0/1/2/3	Mucientes sub-translucent silcrete	Sub-translucent to sub-opaque, grey, light-grey, pale yellow (R92, L90, L92), homogenous and banded structure	(mQ), rhyzolith, terrigenous quartz and calcite relict, skeletal (Gas, Char-G, Char-S), bioclastic, moldic and fracture porosity. Silicified lacustrine limestone	Cenozoic - Neogene - Miocenic - Cuesta facies	Continental, lacustrine
		I2b	0/1/2/3/ 4	Mucientes grey/ black silcret	Sub-opaque to opaque, black to light-grey (N73-T73), homogeneous (epigenetic) brechoid and speckled structures, rhyzolith	(mQ), terrigenous quartz and calcite relict, skeletal (Gas, Char-G, Char-S), bioclastic, moldic and fracture porosity. Fresh (<5mm) or pale yellow neocortex (M77). Silicified lacustrine limestone	Cenozoic - Neogene - Miocenic - Cuesta facies	Continental, lacustrine
		X-I3	0/1/3/4	Cream opaque fossiliferous silcrete	Opaque, grey, rose, pale brown (N71, P71, L70, N75)	Skeletal allochems (Gas, Char-G, Char-S), bioclastic and moldic porosity, fracture filled. Neocortex. Silicified lacustrine limestone		Continental, lacustrine
		I7a	0/1/2/3	Ávila translucent with dentritical inclusions silcrete	Translucent to sub-translucent, homogeneous to brechoid structure, grey to white	CQ/mQ, Ch-LF (15%), Mq (<5%), Of). Terrigeneous quartz (<5%). Grounwater silcrete		Continental, groundwater
		I7b	0/1/2/3	Candeleda translucent with black inclusions silcrete	Translucent grey, very dark grey to black (R73, T73), homogeneous	Terrigenous quartz (<5%), rhizoliths, mineralogy (Ch). Grounwater silcrete	Cenozoic - Cretaceous/ Paleogene - Arkose facies	Continental, groundwater
		G5	0/1	Limãos white silcrete	Sub-translucent to sub-opaque, brechoid to homogeneous strutures, white, pale yellow (K92, L92, T85, M91)	(Op), fenestral porosity, serpentinite intraclasts. Silicified dolocrete	Cenozoic - Neogene - Miocene (?) - Vale Álvaro formation	Continental, groundwater/ lacustrine
		H1	0/1/2	Salamanca/Zamora yellow/orange porcellanite	Opaque, homogeneous ar brechoid structure, yellow, yellow-olive, light-grey very light brown, pale red, olive (M77, N87, K73, L71, N15, P87), homogeneous struture	(Op), terrigenous quartz (<10%). Opale with terrigenous quartz. Groundwater porcellanite silcretes with pedogenetic evolution	Mesozoic - Early Cretaceous	Continental, groundwater
		H2	0/1/2	Grey, Salamanca/ Zamora yellow to orange quartzitic silcrete	Opaque to sub-opaque, yellow, grey, red, brown, yellow–red, very light brown, pale red, light red, pink (N73, L30, S15, P70, N65, L71, N15, R13, M15)	Sandstone with opal matrix. Grounwater quartzitic silcrete with pedogenetic evolution	Mesozoic-Early Cretaceous	Continental, groundwater
?	**JV**	**X-J1a**	?	Brown/yellow jaspe vein	Opaque, brechoid and laminated structure, dark brown-grey, dark brown, strong brown (S71, R71, S30, P65)			Continental epithermal
?	**FQV**	**L1**		Marofa brown ferruginous	Opaque, homogeneous, brechoid, brown, strong brown			Continental, groundwater?

(*continued on next page*)

Table 1 (*continued*)

Genetic	CA variable	Code	Gytology		Description	Mineralogy/Porosity/ Allochems	Precursor	Environment
				siltstone and claystone				
Hydrothermal veins		**J1b**	0/1	Almeida brown/ yellow hydrothermal micro-quartz vein	Opaque, brechoid struture, yellow-olive, dark brown-grey, dark brown, strong brown (N89, S71, S30, P65)			epithermal
		J1c	0/1/4	Moncorvo brown hydrothermal micro-quartz vein	Opaque, brechoid structure, dark brown (R75)			epithermal
		J2	0/1	Horta da Vilariça grey to green hydrothermal vein	Sub-opaque to subtranslucent, homogeneous structure, grey to light green. Hydrothermal vein			epithermal
		J3/4	1/2/3/4	Beira red micro-quartz/chacedony vein	Opaque, red to pale red (R13, P20), homogeneous and laminated structure, hydrothermal silica vein		Red microquartz and chalcedony in secondary position	epithermal
		J6	0/1	Morais massif hydrothermal opal	Translucent grey-pink, grey to brown (M30, P30), opaque red (S17) homogeneous to laminated structure	Mineralogy (Ch, Op)	Peridotite, red & translucent opal & chalcedony	epithermal
		J7	0/1	Beira Alta white/ cream/grey microquartz/ chalcedony hydrothermal vein			White/cream/ grey microquartz/ chalcedony	epithermal
		J8	0/1/2	Euhedral smoky quartz				epithermal
	LQV	**J9**	0/1/2/3/ 4	Anhedral milky and grey quartz				epithermal
		J10	0/1/2/3/ 4	Anhedral translucent to clear quartz				epithermal
		J11	0/1/2/3/ 4	Anhedral zoned translucent to clear quartz				epithermal
		J12	0/1/2/3/ 4	Anhedral grey zoned quartz				epithermal
		J17	0/1	Anhedral smoky quartz				epithermal
	LRC	**J13**	0/1/2/3/ 4	Euhedral translucent to clear quartz				epithermal
		J14	0/1/2/3/ 4	Euhedral milky quartz				epithermal
Igneous rock	**LBR**	**J15**	0/1/2/3/ 4	Rhyolite				
		J16	0/1/2/3/ 4	Basalte				
Hydrothermal vein	**HQ**	**J18**	?	Glossy white quartz				epithermal
	FQV	**J19**	?	Pinky translucent quartz				epithermal
Metasediments	**OQ**	**K**	0/1/2/3/ 4	Ordovician quartzite				marginal marine
	FQV	**M1**	0/1/2/3/ 4	Black fine hornfels				Base of continental slope
	FQV	**N1**	0/1/2/3/ 4	Lydite/Phtanite				Base of continental slope

carbonate rocks (Flügel, 2010) to identify the depositional environments of the siliceous rocks found at Côa Valley Upper Palaeolithic sites (Mangado Llach, 2005; Aubry et al., 2012, Aubry et al., 2014, Aubry et al., 2016b). The systematic macroscopic examination was complemented by a petrographic analysis (mineralogy, texture, and fossil content) of archaeological and geological samples collected and described from the different sedimentary basins (Mangado Llach, 2005).

Survey has been orientated using geological data provided by the Instituto Geológico e Mineiro de Portugal (Carta Geológica de Portugal, Scale 1:50,000), for the West Portuguese Meso-Cenozoic border, in Portugal, and the Instituto Geológico y Minero de España (Mapa Geológico de España, Scale 1:50,000), for the Tagus and Duero basins in Spain. The samples were described, following the genetic and geomorphological description proposed by Fernandes et al. (2008), in terms petrography for the regional lithic resources and of texture and structure, mineralogical and palaeontological content for extra regional flint and silcretes, defining 44 categories (Mangado Llach, 2005; Aubry et al., 2012, Aubry et al., 2014, Table 1). The sample sources were plotted on a GIS project, using a SRTM 90 DEM from which distances and least-cost paths were calculated (Aubry et al., 2016b).

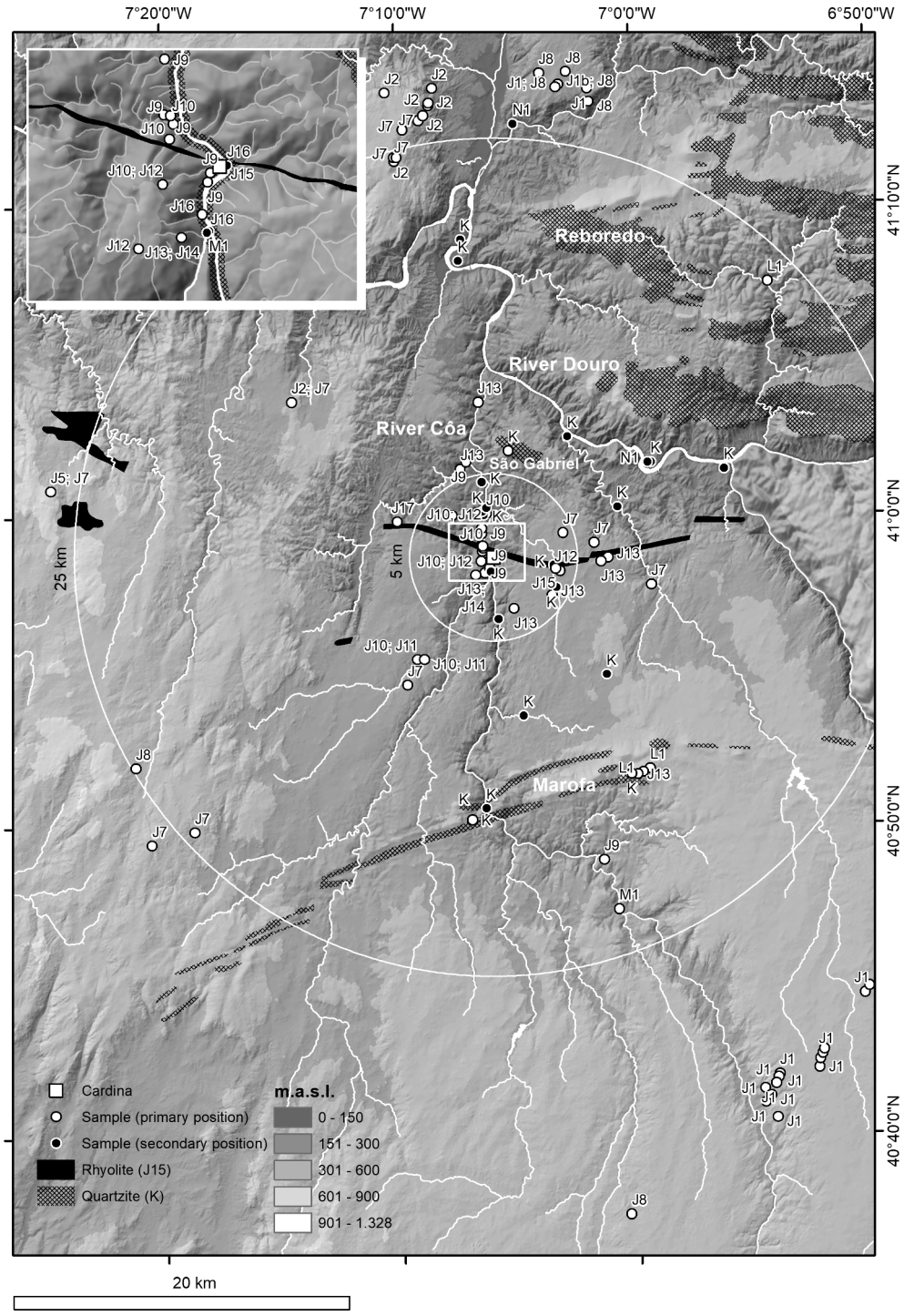

Fig. 4. Location of the sampled quartz vein categories (J1-J17) and quartzite (K) of the Côa Valley study area defined in Table 1.

For both regional and extra-regional origins, lithic assemblages have been classified in technological classes corresponding to reduction sequences, starting with blocks, fragments from veins of siliceous rock, nodules or pebbles, to establish the production processes represented for each different raw material, their techniques and purposes and blank selection for retouched tools following the chaîne opératoire approach (Leroi-Gourhan, 1964) to assess the reduction sequences and their representativity in the excavated areas (Demars and Laurent, 1992; Hofman and Enloe, 1992; Boëda, 1993; Dibble and Bar-Yosef, 1995; Pelegrin, 1995; Zilhão, 1997; Mourre, 2003; Terradas, 2003).

In order to identify the main trends across time, but also eventual patterns in space, we have performed a correspondence analysis (CA) for the Cardina-Salto do Boi lithic raw materials assemblages, which was followed by its hierarchical clustering, using R Language (R Core Team, 2013) and its package FactoMineR (Husson et al., 2018). The resulting graphs were then reworked in Illustrator CS3 to enhance their legibility. The lithic assemblage of each GFU of the four excavated sectors (H'/I', N/O, U, Z/A', Fig. 2) was considered as an individual.

Each variable is composed of several raw material categories that are grouped according to its geological characteristics (Table 1) and the location of its nearest sources from the Cardina-Salto do Boi site (see Figs. 4, 6). The 10 groups and its respective codes (Tables 1, 2) are:

Fig. 5. Geological samples of the categories J1b-Brown micro-quartz, J2-Green epithermal micro-quartz and chalcedony; J5-Yellow opal; J7-Epithermal micro-quartz and chalcedony; J8-Euhedral smoky quartz; J9-Anhedral milky quartz; J10-Anhedral translucent to clear quartz; J11-Anhedral zoned translucent to clear quartz; J12-Anhedral grey zoned quartz; J13-Euhedral translucent-clear quartz; J14-Euhedral milky quartz, J17-Anhedral smoky quartz, M1 - hornfels, L1 - ferruginous siltstone and claystone (see description in Table 1).

Central Portugal flint and silcrete (CP), Duero Basin silcrete (DB), Jasper vein (JV), Fine-grained quartz and chalcedony vein, ferruginous siltstone (FQV), Local quartz vein and specific quartz vein and rock crystal (LQV), Local rock crystal (LRC), Local basalt and rhyolite (LBR), Heated quartz (HQ), Ordovician quartzite (OQ) and undetermined. The last group was not included in the analysis. GFU_UA's with less than twenty pieces, as well as the ones attributed to the Holocene (GFU_UA's 3), were included only as supplementary individuals and not considered in the hierarchical clustering analysis.

4. Results

4.1. Local and regional siliceous rocks

The study area is located in the Palaeozoic Iberian Massif of Central Iberia, and more specifically in the northern sector of the Central Iberian Geotectonic Zone, part of the Iberian Peninsula that constitutes a large outcrop of the old European Variscan Chain (Ribeiro, 1974, 1981; Ribeiro et al., 1979). The region is featured by the extension of metamorphic outcrops consisting of intensely folded and faulted phyllite, greywacke and quartzite, from the Precambrian to the Ordovician

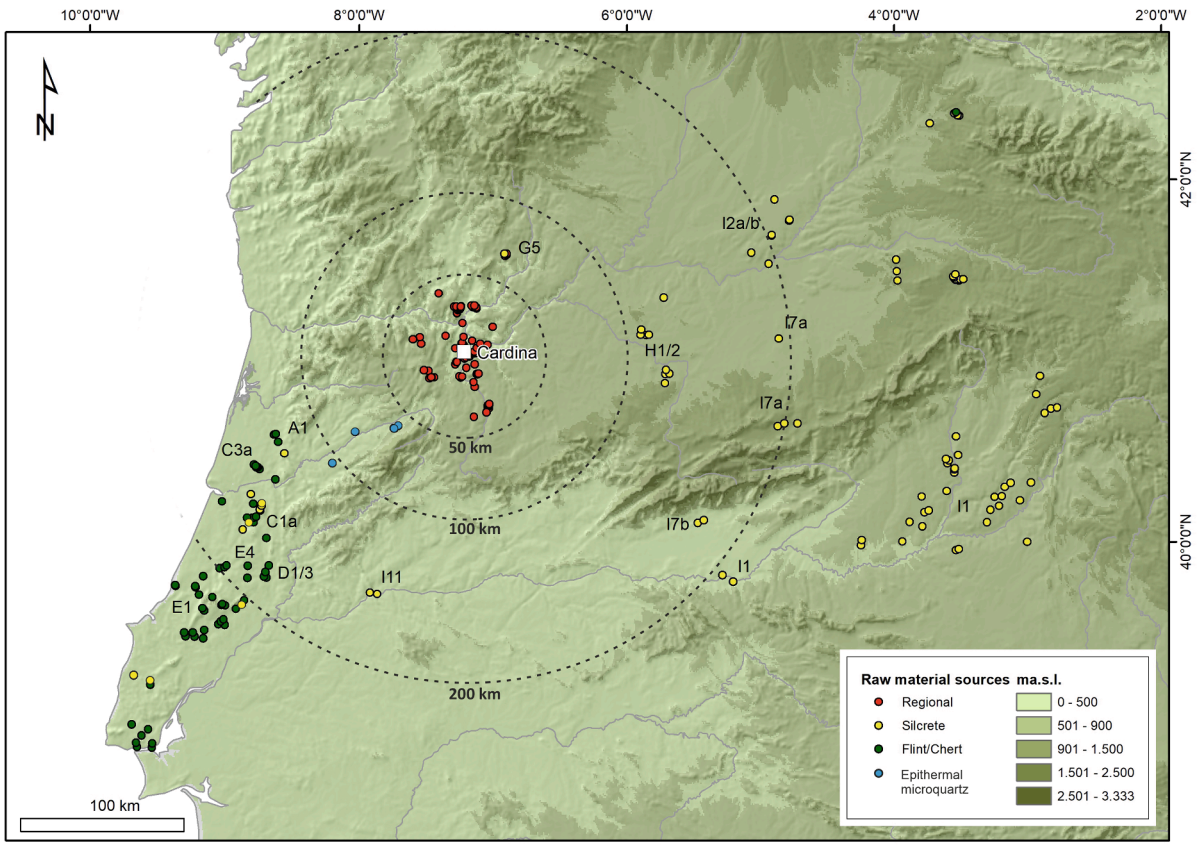

Fig. 6. Regional, flint and silcrete sources (see codes conventions in Table 1) sampled and described.

(Ribeiro, 1974; Silva et al., 1989; Ribeiro et al., 1990; Silva and Ribeiro, 1991; Ribeiro, 2001; Pereira, 2001) intruded by Hercynian granites (Cabral, 1989; Silva and Ribeiro, 1991; Carvalho, 1992; Ribeiro, 2001).

Ordovician quartzite ridges are the main regional landforms and both granitic and metasedimentary rocks display important fault systems filled by quartz, pegmatite, basalt, and rhyolite veins, following the main regional tectonic structures. Metamorphic and granitic rocks are buried by Paleogene, Neogene, and Quaternary siliciclastic deposits.

In this region, the most frequent forms of vein and dike filling are anhedral milky quartz (J9, Fig. 4), translucent anhedral quartz (J10), and zoned translucent anhedral quartz (J11) resulting from tectonics, or grey quartz (J12). All these quartz varieties are widely available as vein outcrops, frequently fractured by tectonics, or as eroded fragments in slope or alluvial deposits around the Cardina-Salto do Boi site. Translucent (J13) and milky euhedral quartz (J14) have a more restricted location, associated with previously mentioned anhedral translucent and milky quartz dike and vein filling (Fig. 4).

Ordovician quartzites are exposed in folded structures constituting the reliefs of Marofa, São Gabriel and Serra do Reboredo (Fig. 4). This raw material is also available as cobbles and boulders in secondary position in the siliciclastic Pliocene deposits, covering the Meseta erosion surface, and in the Quaternary fluvial deposits (Fig. 4). Epigenetic evolution between the genetic types of Ordovician quartzite outcrops and rounded fragments in conglomerate and siliciclastic Cenozoic deposits have been observed, depending on the geochemical environment and distance from the Ordovician outcrops, like those described in Cantabria (Prieto et al., 2021).

Other types of raw materials such as epithermal micro-quartz and chalcedony (J1b, J2, J7), and smoky euhedral quartz (J8) have been detected in the region (Fig. 5), as fracture and fault vein filling, in direct association with the Beiras' uranium and gold deposits, related to uranium-bearing Variscan granites (Neiva, 2003; Aubry et al., 2014, Aubry et al., 2016a). The different types of uranium deposits associated with quartz and jasper veins have been studied in detail (Neiva, 2003). Two specific varieties of micro-quartz and chalcedony vein filling, geographically restricted, used in lithic industries have been detected during the survey. The brown epithermal micro-quartz (J1b), associated with the breccia uranium deposits (Neiva, 2003, Figs. 4, 5), has been detected between Almeida and Ribeira dos Tourões uranium mines and near Estevais. The existence of archaeological remains associated with J1b outcrops, recovered during the geological survey in the first area, and binocular examination suggest a supply from the southern sources. The second vein variety is a green micro-quartz and chalcedony (J2) that has only been detected north of the Douro valley in the vicinity of Horta da Vilariça, is associated with a fault parallel to the Vilariça Fault, a main tectonic feature in Portugal (Figs. 4, 5).

A large porphyritic rhyolite dike (J15) with E/W direction, which can be observed along 20 km in the region, crosses the Côa valley at the Cardina-Salto do Boi site (Fig. 4). This rock is available locally on the site or as pebble, downstream, in the Côa River terraces and alluvial deposits. Other fine-grained siliceous rocks are attested archaeologically, like the ferruginous siltstone and claystone that has been detected in the Marofa Mountain (L1), the siliceous hornfels resulting from contact metamorphism of Palaeozoic rocks around granite intrusions in the Côa Valley (M1) and the Silurian lydite and phtanites available in the Rio Douro and Rio Sabor fluvial terraces (N1) (Figs. 4, 5).

The equivalent to the brown-reddish jasper (X-J1a), identified in the archaeological lithic assemblages in the Côa Valley (Aubry et al., 2012), has not been found during the survey. However, this lithic raw material presents some petrographic characteristics similar to the J1b type, which suggests the same association with a regional uranium vein.

Table 2
Lithic raw material variables (see Table 1 and Figs. 4, 5, 6) used for the Correspondence Analysis of the knapped lithic materials assemblages by UA/GFU 4 to 7 from 4 excavated areas (N/O, 15/17, U-15/16, Z/'A-6/8, H'/I'-17–19).

GFU_UA	A-E *CP*	H1-2, I1-5, 7, 11 *DB*	X-J1a *JV*	J1b, J2, J4-8, J18, L1, M1 *FQV*	J9-12, 17, 19 *LQV*	J13-14 *LRC*	J15-16 *LBR*	J18 *HQ*	K2 *OQ*	Undet.	*Total*
3	2	6		3	579	22	6		36	5	*659*
4_01	1	5		6	538	23	8	1	42	3	*627*
4_02	5	14	1	11	706	42	15	1	102	5	*902*
4_03	11	15		12	826	43	17	1	113	6	*1044*
4_04	14	12		20	890	53	32	1	118	4	*1144*
4_05	13	12		6	531	29	20		84	6	*701*
4_06	3	2	2	4	190	8	3		24		*236*
4b_01	15	17		10	717	36	20		162	3	*980*
4b_02	17	40	1	16	784	43	26		163	2	*1092*
4b_03	17	34		11	998	63	23		167	1	*1314*
4b_04	9	21	2	12	523	31	9		104		*711*
4b_05	1	1		1	81	8	5		14	6	*117*
5_01	8	16	1	3	344	27	4		35	2	*440*
5_02	17	34	3	11	818	45	10		97		*1035*
5_03	21	27	2	7	786	43	8		82		*976*
5_04	12	17	2	9	568	56	13		48	2	*727*
5_05	9	13	4	5	471	45	6		28		*581*
5_06	4	5	3	2	418	28	2		21	2	*485*
5_07	3		6	1	395	16	2		4	1	*428*
5_08	3	3	1	3	316	14	4		13		*357*
5_09		2	3		373	4	1		2		*385*
5_10	2	1	1		325	6			4		*339*
5_11					340	4	2		2		*348*
5_12	1	1			641	9	5		8		*665*
5_13		1			159	8	2		1		*171*
5_14			1		259	4	2		1		*267*
5_15	1				206	5		2	1		*215*
5_16					285	16	2	1			*304*
5_17					229	9	1				*239*
5_18					302	11	3	1	1		*318*
5_19					282	3					*285*
5_20					262	3	2				*267*
5_21					189	2	1				*192*
5_22					330	7	3	6			*346*
5_23		1			225	2	1	5	2		*236*
5_24					307	9	2	14	1		*333*
5_25					261	4	1	51			*317*
5_26				1	318			45	2		*366*
5_27					284			43	1		*328*
5_28					242	1		25	3		*271*
5_29					238	2		21	1		*262*
5_30					226			15	2		*243*
5_31					171	2		13			*186*
5_32					154	1		4			*159*
5_33					120			2			*122*
5_34					107	1	1	3			*112*
5_35					93	1		1			*95*
5_36					59	1		1	2		*63*
5_37					65	1		1	1		*68*
5_38					38			2			*40*
6_01					4						*4*
6_02					1						*1*
6_03					1						*1*
6_04											
6_05					3						*3*
6_06					2						*2*
7_01					1						*1*
7_02					2				2		*4*
7_03					9						*9*
7_04					8						*8*
7_05					18						*18*
7_06					10		1				*11*
7_07					7						*7*
7_08					7		1				*8*
7_09					2		2				*4*
7_10					4						*4*
7_11					4		1				*5*
Total	*189*	*300*	*33*	*154*	*18,652*	*791*	*267*	*260*	*1494*	*48*	*22,188*

Z/A' 6/8

GFU_UA	A-E	H1-2, I1-5, 7, 11	J1a	J1b, J2, J4-8, J18, L1, M1	J9-12, 17, 19	J13-14	J15-16	J18	K2	Undet.	*Total*

(*continued on next page*)

Table 2 (*continued*)

GFU_UA	A-E *CP*	H1-2, I1-5, 7, 11 *DB*	X-J1a *JV*	J1b, J2, J4-8, J18, L1, M1 *FQV*	J9-12, 17, 19 *LQV*	J13-14 *LRC*	J15-16 *LBR*	J18 *HQ*	K2 *OQ*	Undet.	*Total*
	CP	*DB*	*JV*	*FQV*	*LQV*	*LRC*	*LBR*	*HQ*	*OQ*		
3	13	9		11	1919	207	13	4	196	49	*2421*
4_01	15	12		7	933	146	17		112	5	*1247*
4_02	4	17		5	737	55	16		109	6	*949*
4_03	12	22		8	784	56	22	7	144	9	*1064*
4_04	5	46		16	1446	139	37	6	313	6	*2014*
4_05	11	63	1	19	1567	134	41	3	328	5	*2172*
4_06	14	37		17	1274	77	21	2	303	27	*1772*
4_07	17	74	2	12	1480	103	45	15	440	2	*2190*
4_08	11	59	1	20	1553	105	45	5	456	7	*2262*
4_09	23	45	1	18	1213	106	31		225	3	*1665*
4_10	7	25	2	10	817	75	26	3	175		*1140*
4_11	11	37		16	809	55	11		156		*1095*
4_12	11	24	1	7	600	39	8	2	102	2	*796*
4_13	3	28		3	600	44	13		91	2	*784*
5_01	4	12		5	284	16	3		87	3	*414*
5_02	9	39	5	8	1072	66	19	3	212	8	*1441*
5_03	8	30	1	7	946	77	14		99	6	*1188*
5_04	3	26		4	767	42	17		95	8	*962*
5_05	6	19	2	1	468	35	6		38	6	*581*
5_06	3	4	1		258	8	2		11	1	*288*
5_07		2		2	326	12	1	1	17		*361*
5_08		2		2	239	7	3		9		*262*
5_09		1			222	5	1		6	1	*236*
5_10		1			226	7			1		*235*
5_11		2	1		247	1			1		*252*
5_12		1			251	1					*253*
5_13	1				180	1			2		*184*
5_14					223	1					*224*
5_15					113	4					*117*
Total	*191*	*637*	*18*	*198*	*21,554*	*1624*	*412*	*51*	*3728*	*156*	*28,569*

N/O 15/17

GFU_UA	A-E *CP*	H1-2, I1-5, 7, 11 *DB*	X-J1a *JV*	J1b, J2, J4-8, J18, L1, M1 *FQV*	J9-12, 17, 19 *LQV*	J13-14 *LRC*	J15-16 *LBR*	J18 *HQ*	K2 *OQ*	Undet.	*Total*
5_01	20	45	9	28	1126	248	7		333	9	*1825*
5_02	4	31	2	9	826	189	6	1	171	2	*1241*
5_03	6	34	1	6	894	163	8		273	3	*1388*
5_04	14	25	5	6	868	112	5	3	240	2	*1280*
5_05	10	19		6	776	72	7	4	211	2	*1107*
5_06	8	18		6	815	56	5	3	141	2	*1054*
5_07	2	13		4	344	31	1	1	39	1	*436*
5_08		9		5	273	17	2	5	26		*337*
5_09		5			247	13		3	12		*280*
5_10		1			194	13		8	6		*222*
5_11		1			144	5		3			*153*
5_12					166	4	2	2			*174*
5_13		1			181	4					*186*
5_14					236	11		5	2		*254*
5_15					87			1			*88*
5_16					165	1		1			*167*
5_17					150	3		1			*154*
5_18					100			3	1		*104*
Total	*64*	*202*	*17*	*70*	*7592*	*942*	*43*	*44*	*1455*	*21*	*10,450*

U 15/16

GFU_UA	A-E *CP*	H1-2, I1-5, 7, 11 *DB*	X-J1a *JV*	J1b, J2, J4-8, J18, L1, M1 *FQV*	J9-12, 17, 19 *LQV*	J13-14 *LRC*	J15-16 *LBR*	J18 *HQ*	K2 *OQ*	Undet.	*Total*
3	12	16		11	909	75	10	2	118	17	*1170*
4_01		2		3	102	17	15	1	75	5	*220*
4_02		6		2	292	10	4	2	94	7	*417*
4_03	9	11	2	7	279	19	11		87	8	*433*
4_04	8	25		16	455	31	30		120	16	*701*
4_05	13	17	3	1	558	25	32		229	22	*900*
4_06	20	51	3	12	1101	43	33	7	452	12	*1734*
4_07	14	14		11	790	28	26	1	290	17	*1191*
4_08	44	40	1	36	1179	64	34	6	477	34	*1915*
5_01	10	22	2	15	449	19	15		136	21	*689*
5_02	19	18		11	476	44	19		168	13	*768*
5_03	5	17	1	15	438	30	15		116	18	*655*
5_04	5	3		3	168	15	4		54	6	*258*
Total	*159*	*242*	*12*	*143*	*7196*	*420*	*248*	*19*	*2416*	*196*	*11,051*

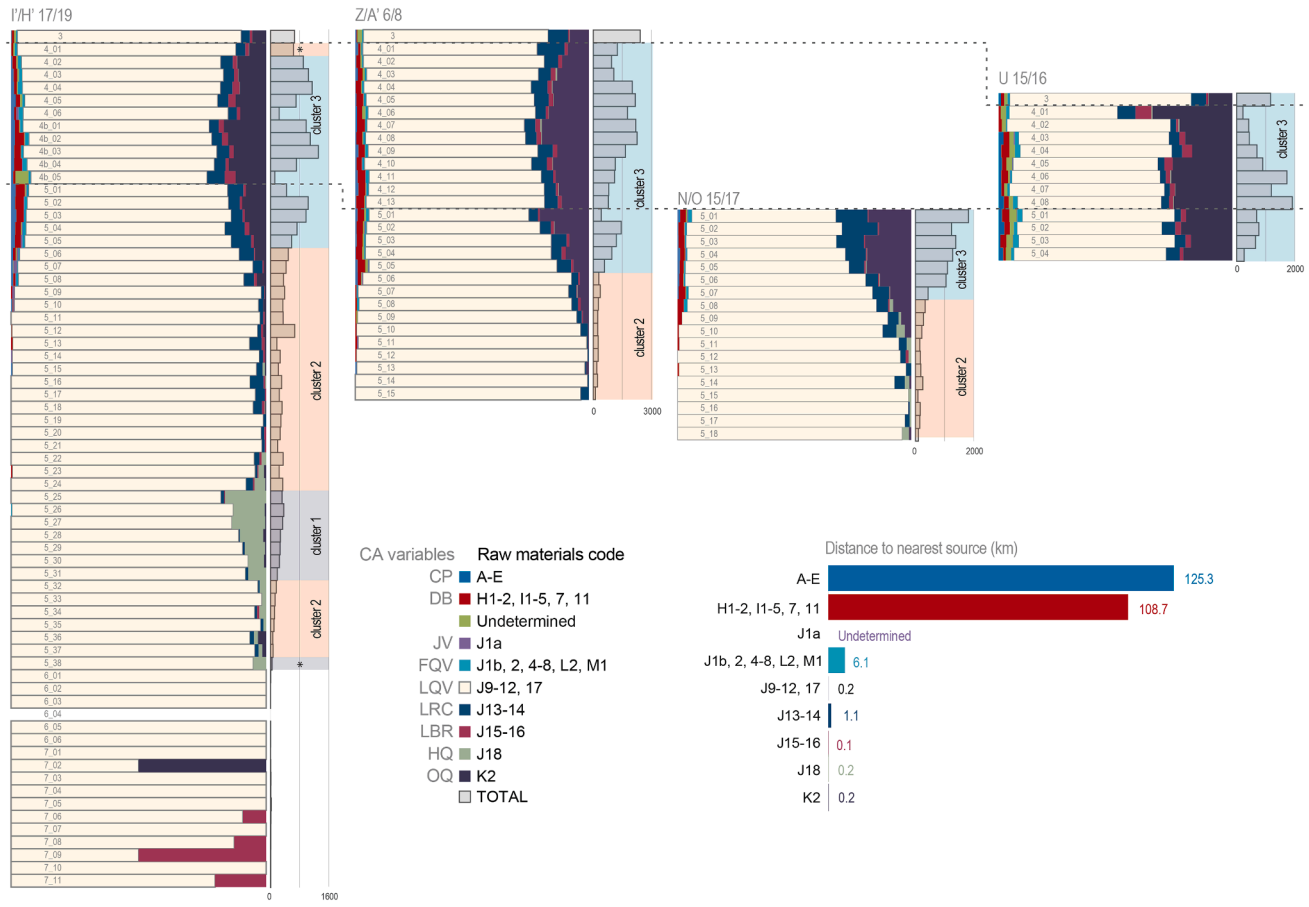

Fig. 7. Lithic remains proportion of pieces by lithic raw material groups along the GFU/UA stratigraphy and clusters defined by the hierarchical clustering analysis in the four areas excavated. Distance from Cardina-Salto do Boi to the nearest source of each group.

4.2. *Extra regional lithic raw materials*

The study of the Cardina-Salto do Boi lithic assemblages recovered between 2014 and 2019 have confirmed the existence, in low percentage, of flint and silcretes from long-distance sources in Mesozoic and Cenozoic formations from Central Portugal and the Duero and Tagus basins, in Spain. (Tables 1, 2, Fig. 6). Survey has confirmed that those sedimentary siliceous rocks formed in marine or continental depositional environments (Mangado Llach, 2005, 2004; Aubry et al., 2012, Aubry et al., 2014, Aubry et al., 2016b) are absent from the regional geological context

4.3. *Raw-material sources and stratigraphical distribution*

The pieces and weigh vertical distribution by area and GFU and 5 cm thick UA reveal that Local quartz vein and specific quartz vein and rock crystal group (CA variable LQV) dominates all the assemblages (Table 2, Fig. 7). J9, J10 and J11 types of vein quartz, available at less than 1 km from the site, represent more than 50% in all the assemblages studied (Fig. 8). Three types of raw material, J12, 17 and 19, are also included in this group. They come from very specific sources located in a radius of 5 km of the site. A specific form of white glossy quartz (J18, Fig. 9, no. 7, 8), probably resulting from accidental heating of J10 or J11 quartz vein, described experimentally as the bleaching process of translucent quartz by Driscoll (2010) is attested in some UAs of the Middle Palaeolithic sequence in the H'/I' area.

Ordovician quartzites (OQ) obtained as pebbles in the Côa fluvial deposits (K, Fig. 4), or more rarely in the Pliocene deposits covering the *Meseta* surface, is present in low proportions in GFUs 5, 6 and 7 (Fig. 7, Table 2). However, the percentage of this raw material increases significantly in the lithic assemblages recovered at the top of the GFU 5, attaining ~20% in GFUs 4 and 4b.

Despite its availability just near the site, porphyritic rhyolite was scarcely used throughout all the Middle and Upper Palaeolithic sequence. This raw material was grouped with basalt, available as pebbles in coarse fluvial deposits, forming the CA variable Local basalt and rhyolite (LBR).

Likewise, although Local rock crystal (LRC) is present in low proportions (<5%) in most of the 5-cm thick UAs, there is a clear increase after the GFU5, namely in UA7 (N/O-15/17), UA5 (A'/Z-6/8), and UA6 (H'/I'- 17/19), as well as in GFUs 4 and 4b (Fig. 8, no. 1–3).

The raw material that constitutes the variable fine-grained quartz vein (FQV) are only present above GFU 5/UA14 (area H'/I'), GFU 5/UA11 (Z/A') and GFU 5/UA13 (N/O), making less than 5% of the assemblages. These raw materials come from different regional sources.

Flint and silcretes from Central Portugal (CP) and the Duero Basin (DB), either formed in marine or continental sedimentary environment (Table 1, Fig. 6, Aubry et al., 2012, 2016b; Mangado Llach, 2005; Aubry et al., 2014) are only present above the GFU 5/UA15, and in GFUs 3, 4 and 4b (Table 2).

5. Archaeological interpretation of the multivariate analysis

The first two dimensions of the CA explain 81, 20% of the variability of the sample. Local quartz vein (LQV) is the most conspicuous variable and as such is located near the crossing of the axis of the factorial map (Fig. 10). Heated quartz (HQ) is located at the upper left corner of the graphic, its high frequency being one of the characteristics of one cluster (see below). All other variables are located on the positive side of dimension 1, although only one of these (JV) is on the negative side of

Fig. 8. Cardina-Salto do Boi, GFU 4B (no. 1, 2, 5), GFU 5 (3, 4, 6–12)., GFU 7 (13), J13-euhedral transparent quartz (no. 1,3–6, 10–12), J8-Euhedral smoky quartz (no.2), J18-glossy white quartz (no. 7), J9-Anhedral milky and grey quartz (no. 8); J11-Anhedral zoned translucent to clear quartz (no. 9) and J17-anhedral smoky quartz (no. 13).

dimension 2. Basically, the graphic shows a huge contrast between the assemblages dominated exclusively by local raw materials (negative side of dimension 1) and those with higher percentages of regional and extra-regional raw materials, as well as quartzite (OQ). The isolation of jasper vein (JV) is, however, very explicit and requires further explanation (see bellow).

The hierarchical clustering analysis suggests the existence of 3 clusters (Fig. 10**,** Supplementary Fig. 1 e 2).

Cluster 1 is characterized by its frequency of HQ, which is higher than the overall mean of the site, by the scarcity of FQV, LBR, LRC and OQ and absence of CP and DB (Supplementary Table 1). It is restricted to GFU's H'/I'_05_25 to 31 and H'/I'_5_38.

Cluster 1 coincides grosso modo with the group of GFU's where a very specific reduction sequence was identified (UA_24 to 29). This reduction sequence corresponds to the production of small quadrangular flakes and possibly bladelets on prismatic cores (Fig. 9). One flake produced by this reduction method has been truncated (Fig. 9, no. 8). An OSL age of ca. 80.3 ± 3.6 Ka is associated with this cluster (Fig. 3, Aubry et al., 2020). The inclusion of H'/I'_5_38 is explained by its few pieces (only 40, it is the layer with lesser pieces included in the analysis) and few varieties of raw materials, it being one of the two layers included in the analysis with only two types of raw material.

Cluster 2 is characterized by a high frequency of LQV and poor representations of the remaining lithic raw materials (Supplementary Table 1). The cluster is composed by all artificial units of GFU 5 not included in the previous cluster that are older than (and including) artificial units 6 of sectors Z/A' and H'/I' and 8 of area N/O. It also includes artificial unit 1 of GFU 4 of the H'/I' sector.

The most frequent method of lithic production identified in cluster 2 corresponds to pseudo-Levallois triangular and flakes produced by prismatic, discoid centripetal bifacial or multifacial methods (Terradas, 2003, Fig. 13). Few blanks were retouched into single, double, or convergent side-scrapers, notches, and denticulates.

However, GFU H'/I'_4_01 and the upper units of GFU 5 (H'/I'_5_06 to 8, Z/A'_5_06 to 8 and N/O_5_08) have Palaeolithic lithic technology.

The location of GFU_4_01 can be explained by the intrusion of early Holocene materials. In fact, the GFU_03, although not included in the analysis, is in this sector of the map (Fig. 10). The remaining units with Upper Palaeolithic technology are clearly related with an early phase, as can be shown by the grouping of these units in the same branch of cluster 2 (Supplementary Fig. 1) and by its location on the factorial map (Supplementary Fig. 2). In fact, at least four of these assemblages (H'/I'_5_to 8) contain blades produced on prismatic unipolar cores and prepared by a central cresting and bladelets, exhibiting the

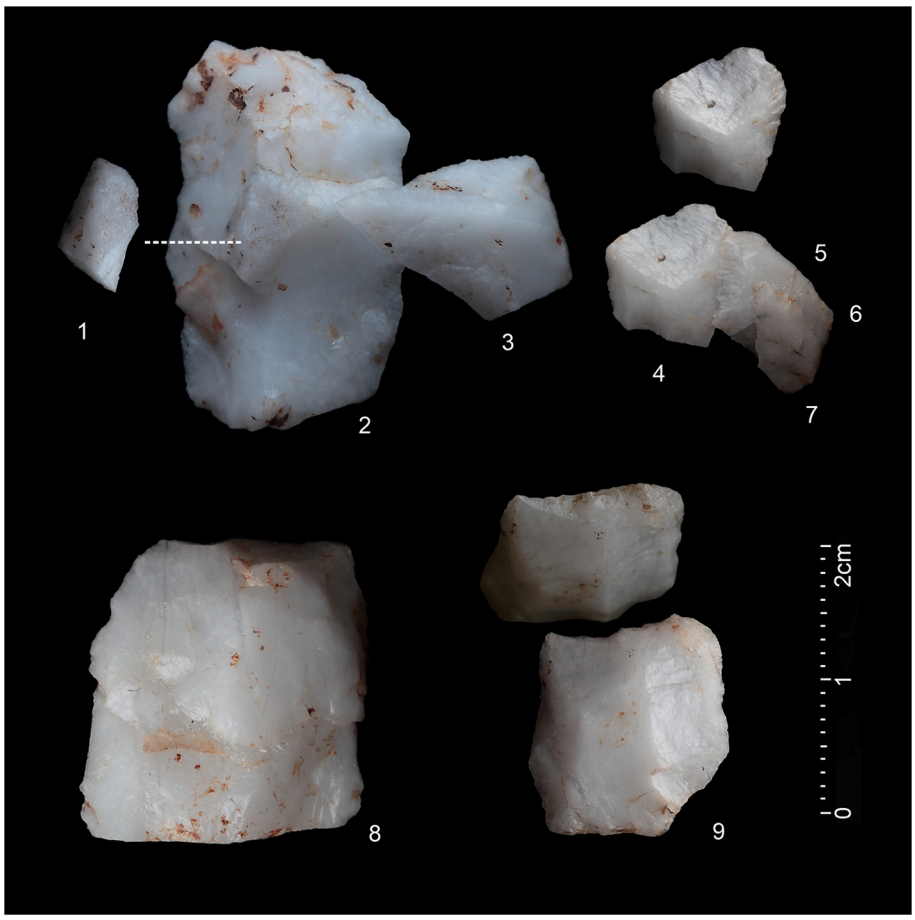

Fig. 9. Cardina-Salto do Boi, J18-Anhedral glossy white quartz. Quadrangular flakes, truncated bladelet and bladelets produced on prismatic cores from GFU 5/ UA24 (no. 5, 6), UA25 (no. 1, 3, 8), UA26 (no. 2, 7), UA28 (no. 4) UA30 (no. 9).

technological characteristics of bladelet production on rock crystal prism termination, burin and carinated nose-scraper core reduction strategy (Fig. 11). A few of these bladelets has been transformed into Dufour bladelets, subtype Dufour and Font-Yves. The first blades appear, however, in older units, namely on GFU H'/I'_14 (Table 3), although this blade fragment is probably intrusive as it is suggested by the stratigraphic distribution of the jasper vein remains (Fig. 11) and refitting set of rock crystal and quartz remains (Aubry et al., 2020). The common feature of the blade reduction sequence is its raw material (JV). This raw material is present in other the Upper Palaeolithic layers, but its relevance is stronger in the older assemblages. This is what explains the position of this variable in the factor map, away from the remaining variables connected with the Upper Palaeolithic and closer to the location of the Early Upper Palaeolithic GFU's of both clusters 2 and 3 (Fig. 10).

Cluster 3 is characterized by high frequencies of OQ, LRC, DB, LBR, CP and FQV as well as comparatively low percentages of HQ and LQV (Supplementary Table 1). This cluster includes all the excavated layers of U area, all the artificial layers between GFU5_01 and GFU 5_07 of the N/O area, all the layers between GFU 5_05 and GFU 4_02 of the H'/I' area and above and including GFU5_5 of the Z/A' area.

All the GFU 5 included layers have yielded retouched bladelets, micro-gravette and backed point fragments, and several Noailles burins (Demars and Laurent, 1992) in the H'/I' area, made from long-distance flint and silcrete sources and regional rock crystal and epithermal microquartz (Fig. 11). Layer 4b lithic assemblage is characterized in the four areas by the presence of backed points, micro-gravette points and retouched bladelet fragments made from local rock crystal the same long-distance sourced flint and silcrete as the top of the GFU 5. Bladelet reduction comprises prismatic, burin core, and bipolar strategies (Fig. 11). The attribution of this cluster to the Upper Palaeolithic is indisputable.

Artificial layers of GFU's 6 and 7 were left out of the analysis because of their low effectives. However, their inclusion, as supplementary individuals, enables us to discuss their location in the factorial map of the CA (Supplementary Fig. 1). GFU 6 and part of GFU 7′ units fall inside cluster 2. However, several units of GFU 7 are set apart because essentially of a higher frequency of LBR. However, the few findings do not allow us to determine if the preference for this raw material, which can be collected on the site itself, is significant or not. Be that as it may, the Levallois centripetal and discoid centripetal methods (Boëda, 1993; Mourre, 2003; Thiébaut, 2013) are the most different methods of lithic reduction identified in both GFU's. Most of the blanks are not retouched and a very low proportion of these flakes has been retouched into notches, denticulates, or single side-scrapers (Fig. 12).

6. Discussion

The first fact that should be noted from the vertical distribution of lithic raw material categories and its multivariate analysis is the rarity of the quartzite in all the assemblages yielding lithic remains with Middle Palaeolithic flake reduction sequences and in the first occupation yielding blade and bladelet reduction sequence of the H'/I' area (clusters 1 and 2). This raw material, well suited to the Levallois and discoid reduction sequence, predominates in large parts of western, central, and northern Iberian Middle Palaeolithic occupations (De la Torre et al., 2013). Quartzite is available as cobble in present-day fluvial deposits of the Côa Valley and attested in the Middle Palaeolithic occupation of the

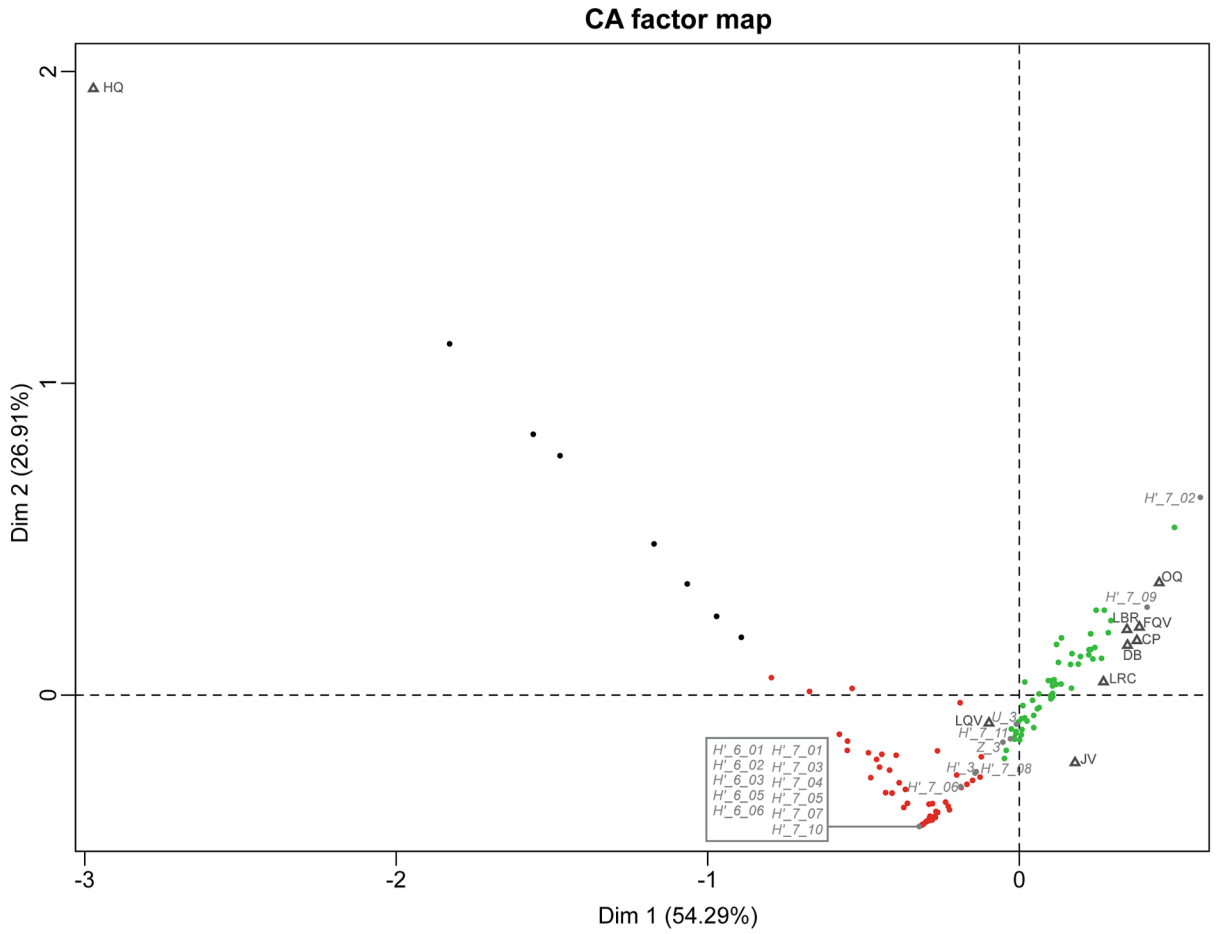

Fig. 10. Distribution of the lithic assemblages of each GFU_UA (dots) and type of raw material (triangles) along the first two dimensions of the Correspondence Analysis. Supplementary GFU Ua's are represented in grey and the GFU of each cluster suggested by the Hierarchical Cluster Classification in a given colour (black: cluster 1; red: cluster 2; green: cluster 3).

granitic plateau (Olga Grande 4, level 5 and 6, Olga Grande 14 level 4, Aubry, 2009, Fig. 1). The preservation of the GFU 5, 6, 7 and 8 fine-grained alluvial deposits, 20 m above the present-day Côa riverbed, could explain this fact if we consider that the cobbles and boulders that constitute the fluvial deposit of high energy depositional environment were buried by the low energy deposits and not accessible during the Middle Palaeolithic and Early Upper Palaeolithic.

The data obtained using raw material match the stratigraphical disconformity observed ~50 cm below the top of GFU 5 in the H'/I' area (Aubry et al., 2020; Dimuccio et al., 2019) and with the GFU/UA yielding the first blade and bladelet reduction sequence of production (Early Upper Palaeolithic branch of cluster 2) (Fig. 11). This transition dates of between 34.0 ± 2.0 ka and 38.4 ± 1.9 ka, from optically stimulated luminescence ages integrated into a Bayesian model (Aubry et al., 2020).

A detailed reconstitution of technological changes that occurred along the GFU 5 sequence is hindered by the fact that disconformities in alluvial processes at Cardina-Salto do Boi have been detected by micromorphology and clay mineralogy (Dimuccio et al., 2019) and evidenced by 3dimensional representation of lithic remains and refitting links (Aubry et al., 2020). Furthermore, the study of Middle Palaeolithic lithic assemblages of Portugal has been developed in regions with local flint sources (Matias, 2016) or adapted to quartzite (Cura and Grimaldi, 2009) and an analytical framework is still missing for the study of quartz for most of the regions (Driscoll, 2010).

At Cardina-Salto do Boi, the GFU 6 and 7 lithic assemblages, resulting from occupations that occurred before the GI 21 (Rasmussen et al., 2014), present some technological characteristics, like the use of Levallois reduction sequence and production of large flakes, that differ from other GFU 5 assemblages. Despite the absence of flint, technological data present some similarities with Gruta da Oliveira's layers 15 to 25, the reference for Middle Palaeolithic occupation of Central Portugal that has been recently redated by U-series using speleothems, coupled with new luminescence ages for sediment infill. Data show that the site's ~6-m-thick archaeological stratigraphy dates entirely within a <30 ka interval, spanning substages 5a-5b of MIS 5, confirming a shift from the centripetal Levallois reduction to discoid and Kombewa debitage during the time interval of late MIS 5 to early MIS 4 (Deschamps and Zilhão, 2018) and that flake-cleavers and bifaces defining the Vasconian facies are restricted to a short interval correlated with Greenland Stadial (GS) 22, 85.1–87.6 ka ago (Zilhão et al., 2021a).

Discoid reduction methods deduced from the lithic assemblage found throughout the GFU 5 Middle Palaeolithic layers in the 3 areas excavated at Cardina-Salto do Boi are widespread in Iberian Late Middle Palaeolithic assemblages and dated to MIS 5a and MIS 4 (Deschamps and Zilhão, 2018). Along the GFU 5 the selection of local translucent quartz, the reduction sequence used, and morphology of the flakes obtained are similar in the three areas where GFU 5 has been excavated (Fig. 13). The low proportion of cores of the lithic assemblages assigned to the cluster 2 and discoid reduction sequence in the 3 areas (Table 3) reveals that most of the flakes have been produced in other places of the site or near the quartz sources. The only significant different units are H_5_24 to H_5_31 (cluster 1). Here, a high proportion of J18 (HQ) differentiates this set of stratigraphic units from the remaining Middle

Fig. 11. Cardina-Salto do Boi, lithic industries and inferred blade and bladelet reduction sequences from GFU 4b, GFU 5 UA1 to 14.

Palaeolithic context. From these units, with an age of 80.3 ± 3.6 Ka obtained by luminescence on deposits recovered from the H_ 5_32 (Aubry et al., 2020), also came the set of small quadrangular flakes and possibly bladelets on prismatic cores (Fig. 9) attested in Middle Palaeolithic occupations of different regions and chronology in Iberia, interpreted an adaptation to raw material constrain (De la Torre et al., 2013). At Cardina-Salto do Boi a relation between Heated quartz and this reduction sequence is thus confirmed.

The GFU 5/UA1-10 lithic assemblages are distinct and can be assigned by their typology and technology to the Early Upper Palaeolithic. Different groups can be defined based on reduction strategies and tool types (Fig. 11). The lithic assemblages recovered in the early Upper Palaeolithic branch of cluster 2 of H'/I'-17/19 area comprises blade fragments and bladelets produced on carinated and burin cores, associated with Roc-de-Combe subtype Dufour and Font-Yves bladelets made from jasper vein from an unknown source, rock crystal, flint and silcrete (Fig. 11). These are typical index fossils of the Evolved Aurignacian (Rigaud, 1982; Demars and Laurent, 1992; Michel, 2010; Rigaud et al., 2016). This attribution fit with the OSL ages of ~33.6 ± 2 ka obtained for sample 17,211 (Aubry et al., 2020). In open-air sites in Central Portugal, blades produced on prismatic unipolar cores and bladelets on burin/carinated cores have been assigned to the Final or Evolved Aurignacian (Zilhão, 1997, 2006; Zilhão et al., 2010; Aubry et al., 2006). This attribution is compatible with the data of southern Iberia (Zilhão et al., 2017; Villaverde et al., 2019) and recently obtained at Caldeirão cave in Central Portugal (Zilhão et al., 2021b).

The attribution of the lithic assemblage from the level GG of Lapa do Picareiro Cave, with a total of 42 flint pieces, mostly composed of twisted or curved bladelets and fragments of bladelets, carinated endscrapers and blades or fragments of blades, to an early Aurignacian

Table 3
Techno-typology composition of the lithic industries by UA/GFU 4 to 7 of the H'/I'-17/19, N/O-15/17, Z/A'-6/9, U-15/17 squares.

H'/I' 17/19	tool	core	blank									*Total*
			fragment	pebble	flake	siret flake	blade	bladelet	burin bladelet	chip	heated fracture	
1	–	–	–	–	1	–	–	–	–	–	–	*1*
2	–	–	2	–	14	–	–	–	–	6	7	*29*
3	10	13	11	2	395	–	2	5	–	225	185	*848*
4_01	4	20	8	–	283	–	1	4	–	312	220	*852*
4_02	14	19	16	2	494	–	2	10	–	352	387	*1296*
4_03	13	18	16	–	493	–	2	20	–	487	328	*1377*
4_04	12	14	12	–	571	–	1	18	–	517	256	*1401*
4_05	10	13	8	–	309	–	3	15	–	346	146	*850*
4_06	2	3	1	–	101	–	–	6	–	123	25	*261*
4b_01	23	18	8	7	353	68	2	23	1	483	300	*1286*
4b_02	16	26	2	10	322	101	7	44	–	572	304	*1404*
4b_03	20	24	3	9	345	101	3	52	–	763	167	*1487*
4b_04	6	8	–	2	150	33	3	22	–	495	61	*780*
4b_05	–	4	–	–	36	–	–	7	–	70	2	*119*
5_01	6	3	1	1	68	17	–	19	–	327	34	*476*
5_02	6	9	1	2	178	40	–	34	–	766	71	*1107*
5_03	11	10	–	4	155	33	2	40	2	720	51	*1028*
5_04	7	9	1	1	113	16	–	33	1	547	68	*796*
5_05	6	5	–	–	79	23	1	32	–	438	62	*646*
5_06	8	4	1	1	70	17	–	19	1	377	47	*545*
5_07	2	3	–	–	75	12	–	10	–	328	45	*475*
5_08	2	1	–	–	57	7	–	7	1	282	30	*387*
5_09	2	1	–	–	82	13	–	6	–	282	21	*407*
5_10	3	1	–	–	82	22	1	5	–	225	13	*352*
5_11	3	1	–	–	75	10	–	1	–	258	50	*398*
5_12	3	2	1	–	112	28	2	6	–	511	120	*785*
5_13	1	2	–	–	40	9	–	6	–	113	40	*211*
5_14	–	–	–	–	47	5	1	1	–	213	28	*295*
5_15	2	–	–	–	41	3	–	1	–	168	68	*283*
5_16	4	1	1	–	74	12	–	–	–	212	120	*424*
5_17	2	1	1	–	49	5	–	–	–	181	86	*325*
5_18	1	3	–	–	72	8	–	1	–	233	103	*421*
5_19	2	1	–	–	95	11	–	2	–	174	92	*377*
5_20	–	2	4	–	71	10	–	–	–	180	62	*329*
5_21	4	4	1	–	55	3	–	–	–	126	57	*250*
5_22	1	2	–	–	52	14	–	1	–	276	35	*381*
5_23	2	2	1	1	75	10	–	1	–	145	15	*252*
5_24	–	1	1	1	73	15	–	4	–	238	32	*365*
5_25	7	4	–	–	72	18	–	8	–	208	29	*346*
5_26	–	1	–	1	69	17	–	5	–	273	26	*392*
5_27	2	1	1	–	46	16	–	4	–	259	14	*343*
5_28	1	3	–	–	53	17	–	5	–	192	18	*289*
5_29	2	–	–	–	42	16	–	3	–	199	7	*269*
5_30	1	1	–	–	36	10	–	3	–	192	21	*264*
5_31	1	1	–	–	28	3	–	3	–	150	8	*194*
5_32	–	1	–	–	27	6	–	–	–	125	7	*166*
5_33	–	–	–	–	22	6	–	1	–	93	–	*122*
5_34	–	–	–	–	9	7	–	1	–	95	1	*113*
5_35	–	1	–	1	19	2	–	–	–	73	–	*96*
5_36	–	–	–	–	17	2	–	–	–	44	3	*66*
5_37	–	1	1	1	12	4	–	–	–	50	2	*71*
5_38	–	–	–	–	9	2	–	–	–	29	5	*45*
6_01	–	–	–	–	3	1	–	–	–	–	1	*5*
6_03	–	–	–	–	1	–	–	–	–	–	1	*2*
6_05	–	1	–	–	2	–	–	–	–	–	–	*3*
6_06	–	–	–	–	1	1	–	–	–	–	–	*2*
7_01	–	–	–	–	1	–	–	–	–	–	–	*1*
7_02	2	–	–	–	1	1	–	–	–	–	–	*4*
7_03	–	–	–	1	8	1	–	–	–	–	1	*11*
7_04	–	–	–	–	7	1	–	–	–	–	–	*8*
7_05	1	–	3	–	13	1	–	–	–	–	–	*18*
7_06	3	–	–	–	8	–	–	–	–	–	–	*11*
7_07	–	–	1	–	6	–	–	–	–	–	–	*7*
7_08	–	1	–	–	5	2	–	–	–	–	–	*8*
7_09	1	–	1	–	2	–	–	–	–	–	–	*4*
7_10	1	–	–	–	3	–	–	–	–	–	–	*4*
7_11	–	–	–	–	5	–	–	–	–	–	–	*5*
Total	*230*	*264*	*108*	*47*	*6284*	*780*	*33*	*488*	*6*	*14,053*	*3882*	*26,175*

Z/A' 6/8	tool	core	blank									*Total*
			fragment	pebble	flake	siret flake	blade	bladelet	burin bladelet	chip	heated fracture	
1_	2	1	1	–	12	–	–	–	–	2	–	*18*

(*continued on next page*)

Table 3 (*continued*)

Z/A' 6/8	tool	core	blank									*Total*
			fragment	pebble	flake	siret flake	blade	bladelet	burin bladelet	chip	heated fracture	
2	–	1	–	–	27	–	–	1	–	9	7	*45*
3	21	42	154	4	772	4	2	43	1	1382	208	*2633*
4_01	8	11	100	9	250	3	–	11	–	859	92	*1343*
4_02	9	9	103	7	231	4	–	13	–	576	78	*1030*
4_03	19	17	106	6	252	3	–	8	1	658	131	*1201*
4_04	24	19	214	9	567	6	–	28	4	1166	273	*2310*
4_05	21	33	187	11	698	20	–	21	4	1212	123	*2330*
4_06	28	29	162	10	556	9	4	33	9	964	133	*1937*
4_07	30	54	181	8	790	12	–	18	5	1101	127	*2326*
4_08	22	40	211	7	908	23	1	21	4	1066	228	*2531*
4_09	10	15	165	9	391	14	1	9	11	1064	94	*1783*
4_10	20	20	112	–	316	20	–	7	2	660	48	*1205*
4_11	6	8	90	3	271	5	–	10	4	710	45	*1152*
4_12	12	4	66	2	179	6	1	7	2	531	19	*829*
4_13	1	5	48	3	200	2	2	9	6	511	20	*807*
5_01	4	8	3	–	218	–	4	11	–	166	41	*455*
5_02	9	18	63	13	359	10	–	16	2	973	76	*1539*
5_03	10	9	52	1	235	4	–	14	4	861	42	*1232*
5_04	5	12	38	5	257	3	–	6	1	642	40	*1009*
5_05	3	2	2	3	90	56	–	12	–	416	23	*607*
5_06	3	1	–	1	29	6	–	4	–	245	13	*302*
5_07	–	5	–	2	25	11	–	6	–	313	11	*373*
5_08	1	2	1	–	16	7	–	6	–	229	1	*263*
5_09	2	1	–	2	47	3	–	3	–	179	17	*254*
5_10	–	5	–	1	53	10	–	2	–	165	13	*249*
5_11	1	2	1	–	57	18	–	–	–	173	8	*260*
5_12	1	2	–	3	58	14	–	2	–	176	15	*271*
5_13	2	–	–	–	30	16	–	2	–	134	13	*197*
5_14	–	1	1	–	52	14	–	1	–	156	7	*232*
5_15	–	1	1	2	41	17	–	–	–	58	7	*127*
Total	*274*	*377*	*2062*	*121*	*7987*	*320*	*15*	*324*	*60*	*17,357*	*1953*	*30,850*
U 15/16	tool	core	blank									*Total*
			fragment	pebble	flake	siret flake	blade	bladelet	burin bladelet	chip	heated fracture	
1_	–	1		–	18	–	–	–	–	4	–	*23*
2	–			–	29	–	–	2	–	8	19	*58*
3	11	30	10	–	562	–	1	35	–	524	206	*1379*
4_01	1	5	1	–	99	–	–	5	–	109	59	*279*
4_02	8	12	7	1	232	–	1	8	–	154	135	*558*
4_03	4	11	2	–	269	–	1	11	–	135	49	*482*
4_04	12	13	5	–	343	–	–	13	–	315	110	*811*
4_05	45	33	11	–	517	–	2	20	–	278	202	*1108*
4_06	22	32	2	–	1136	–	4	28	–	512	232	*1968*
4_07	19	20	2	–	776	–	2	24	–	349	146	*1338*
4_08	29	40	2	–	1235	–	11	51	–	549	190	*2107*
5_01	6	14	1	–	335	–	1	29	–	303	45	*734*
5_02	4	6		–	328	–	1	22	–	407	70	*838*
5_03	5	9	2	–	283	–	1	20	–	336	33	*689*
5_04	3	1		–	132	–	–	14	–	108	7	*265*
Total	*169*	*227*	45	*1*	*6294*	–	*25*	*282*	–	*4091*	*1503*	*12,637*
N/O 15/17	tool	core	blank									*Total*
			fragment	pebble	flake	siret flake	blade	bladelet	burin bladelet	chip	heated fracture	
5_01	2	15	2	–	101	45	–	66	–	1594	24	*1849*
5_02	3	3	1	–	71	25	1	35	–	1102	23	*1264*
5_03	–	8	–	–	129	26	5	36	–	1184	46	*1434*
5_04	1	4	–	1	81	21	–	37	–	1135	21	*1301*
5_05	3	2	1	–	49	15	2	37	–	999	20	*1128*
5_06	3	–	–	–	70	18	–	44	–	919	46	*1100*
5_07	–	5	1	–	39	6	1	14	–	371	19	*456*
5_08	1	2	–	–	51	11	–	5	–	267	40	*377*
5_09	4	3	–	2	47	4	–	2	–	219	61	*342*
5_10	3	2	–	–	37	13	1	2	–	164	34	*256*
5_11	–	3	–	1	31	11	–	1	–	107	33	*187*
5_12	4	–	–	–	31	6	–	–	–	133	30	*204*
5_13	1	–	–	–	35	4	–	1	–	145	19	*205*
5_14	4	1	–	–	49	14	–	–	–	187	56	*311*
5_15	–	1	–	–	28	4	–	–	–	55	23	*111*
5_16	1	3	–	–	30	11	–	–	–	113	10	*168*
5_16?	–	–	–	–	1	1	–	–	–	7	–	*9*
5_17	–	1	–	–	29	8	–	–	–	116	27	*181*
5_18	4	–	–	–	35	9	–	–	–	56	17	*121*
Total	*34*	*53*	*5*	*4*	*944*	*252*	*10*	*280*	–	*8873*	*549*	*11,004*

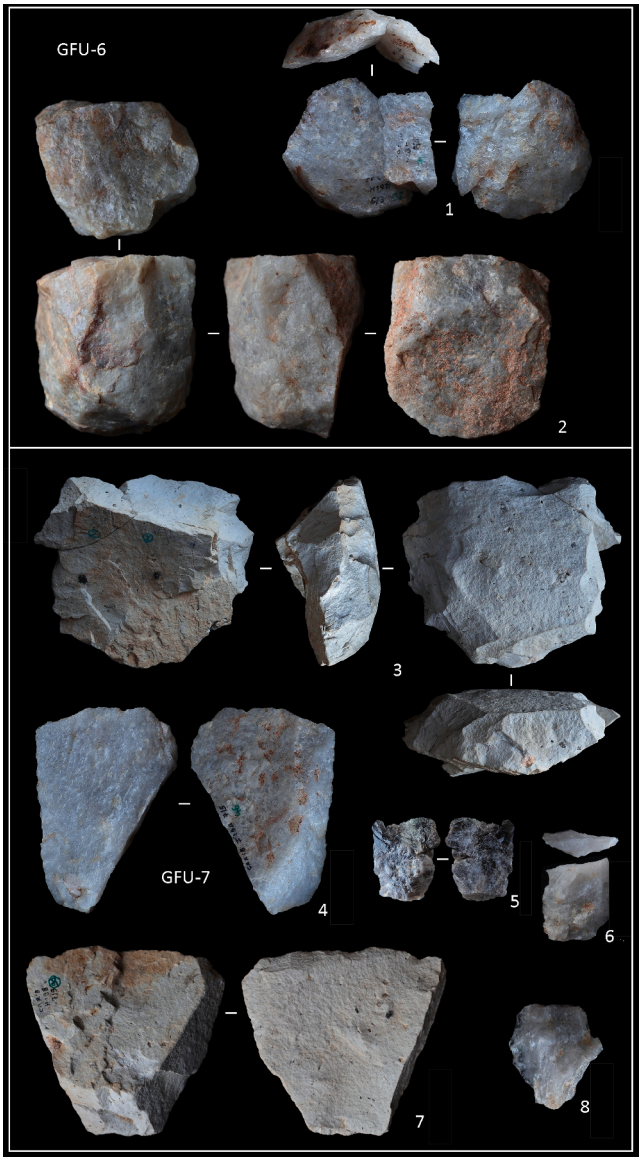

Fig. 12. Cardina-Salto do Boi. lithic industries from the GFU 6 (no. 1, 2) and GFU 7 (no. 3–8).

phase (Haws et al., 2020) or final phase (Zilhão, 2021) is still debated.

The lithic assemblages recovered at the upper top UA's of GFU 5, GFU 4b and GFU 4 can be assigned by typology and technology to different Gravettian phases (Aubry, 2009; Klaric et al., 2009; Aubry et al., 2020). According to its raw material, all but one assemblage of GFU 4 are in cluster 3 (H'/I'_04_01, for reasons explained above). The upper top of GFU 5 is, however, distributed by different clusters. As it was earlier pointed out, GFU 5_5 to 8 of area H'/I', GFU 5_6 to 8 of area Z/A' and GFU 5_8 and 9 of area N/O are the core of the Early Upper Palaeolithic branch of cluster 2. Layers from sector U15/16 are on cluster 3, such as it happens with the remaining layers of GFU 5 of both H'/I', N/O and Z/A' areas. The dispersion of unit with material produced by Upper Palaeolithic blade and bladelet reduction sequences by the two clusters has probably a chronological connotation, given that it is the older layers of each sector that are located on the Early Palaeolithic branch of cluster 2. Only sector U has no units in that cluster because in that area no such old layers were excavated.

In all the three areas, the data recovered from Cardina-Salto do Boi's upper levels characterized by Middle Palaeolithic technology confirm the absence of the bidirectional blade reduction sequence that characterises the Chatelperronian of France (Pelegrin, 1995; Pelegrin and Soressi, 2007; Bachellerie, 2011; Roussel et al., 2016) and Northern Spain (Arrizabalaga et al., 2000; Rodriguez-Hidalgo, 2019), dated of the 44–36 ka cal BP interval (Higham et al., 2010, 2014; Hublin et al, 2012; Talamo et al., 2012; Rodriguez-Hidalgo, 2019), and correlatively proves the persistence of discoid reduction sequence, by this time, in the Côa Valley.

The geographical area defined by the distribution of raw material sources of all the assemblages assigned by their reduction sequence and stone tool types to the Middle Palaeolithic are smaller than all territories defined for Upper Palaeolithic assemblages recovered at the same site, and in the region (Aubry et al., 2012). In regions with flint sources, the study of the origin of flints used by Neanderthal has revealed an extensive knowledge and intensive exploitation of the lithic resources beyond 50 km, with rare displacement of specific flint or silcrete from sources exceeding that distance (Geneste, 1988; Féblot-Augustins, 1999, Fernandes et al., 2008; Turq et al., 2017; Gómez de Soler et al., 2020; Abrunhosa et al., 2020; Prieto et al., 2021). The fact that territories defined by the raw material used for assemblage resulting from occupation yielding discoid reduction sequences of the latest Middle Palaeolithic occupations are even smaller than occupations displaying remains of Levallois technology has been interpreted as an adaptive response to low-quality raw materials, or as a cultural adaptation of the knapping method to high mobility strategies, in distinct environment of France (Delagnes and Rendu, 2011; Thiébault, 2013) or Iberia (Shipton et al., 2013; Romagnoli et al., 2016).

Based on the study of Late Neanderthal skeletal specimens from El Sidrón, in northern Spain, it has been proposed that genetic and skeletal evidence of inbreeding could result of small, isolated groups with potentially high levels of intragroup mating (Ríos et al., 2019). Strontium isotope measurements made by Laser-Ablation ICP-MS along the enamel growth axis of a Neanderthal tooth from Gruta da Oliveira (Central Portugal) recovered in Layer 22, compared with Strontium isotopic mapping of the region have revealed systematic but not seasonal movement from six different Sr catchment areas detected in a range of ~30 km of the Cave (Pike et al., 2016). The lithic assemblage of the layer 22 dated from the end of the Greenland Interstadial 23 (90–92 ka) (Zilhão et al., 2021a) has yielded flint dominated Levallois industry made from sources from the nearby Limestone relief and Tagus valley (Matias, 2016) in the geographic range establish by the Strontium study.

Before accepting that the raw material discarded at Cardina-Salto do Boi is representative of the territories effectively exploited and mobility pattern of all the Neanderthal groups that occupied the site, the first issue will be to evaluate if the absence of regional raw materials in the assemblage of levels 6 and 7, where Levallois reduction sequence is attested, is statistically significant or results from the small area excavated (6 m^2) and the small number of pieces therein identified.

The second issue is to establish if the absence of regional epithermal micro-quartz and chalcedony vein (J1b and J2 included in the FQV variable) and exotic flint and silcrete sources (A, C, D, E, I, H, included in the CP and DB variables), used in low proportion but systematically since the first and during all the Upper Palaeolithic, result from different subsistence-settlement systems (Binford, 1980), social network range (Whallon, 2006) or is related to the suitability of those lithic raw materials for the production of bladelets, during Upper Palaeolithic, or flakes by Levallois or discoid method, for the Middle Palaeolithic.

The green micro-quartz and chalcedony vein (J2), included in the FQV variable, Figs. 4, 5), highly fractured by Hercynian tectonics and available as small quadrangular vein fragments, is attested in all the Upper Palaeolithic occupations (Aubry et al., 2012), Mesolithic and Neolithic (Monteiro-Rodrigues, 2011) for bladelet production (Aubry, 2009), but it is not appropriate for the Levallois and discoid debitage. On the contrary, the J1b brown epithermal micro-quartz (FQV variable), available as large vein fragment (Fig. 5) could have been used to produce flakes.

Nevertheless, in the absence of local and regional flint and silcrete

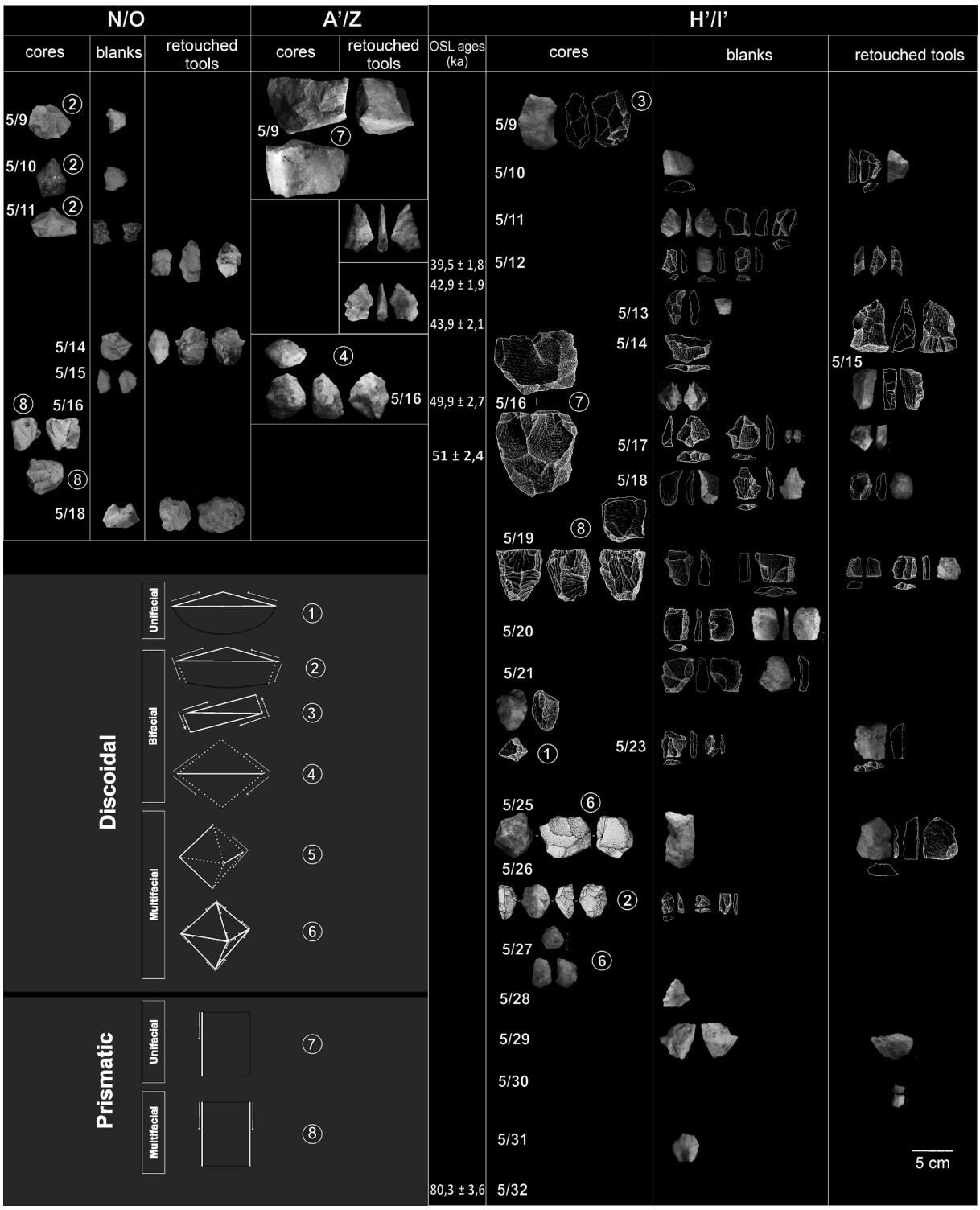

Fig. 13. Cardina-Salto do Boi Lithic industries from the GFU 5 by artificial units (UA9 to 31) and stratigraphical position of the radiometric luminescence data. Cores are classified following the types defined by Terradas (2003).

sources, small tools and bladelet production are attested during the Middle Palaeolithic, associated with the use of heated glossy white quartz that characterizes cluster 3 (Figs. 9, 10). Considering the long chronology of the sequence studied, recovered on four different excavated areas, the use of local quartz vein, small amount of quartzite and the absence of regional epithermal micro-quartz, allochthonous flint and silcrete, can be considered as representative of discoid reduction sequence at Cardina-Salto do Boi.

7. Conclusion

The study of lithic remains from the Middle and Upper Palaeolithic occupations of the Cardina-Salto do Boi open-air site in the Côa Valley, spanning from the MIS 5 to 3, provides new data to infer Neanderthal and AMH land use and social network. Through the stratigraphy, the transition from the Neanderthal-associated Middle Palaeolithic technology to the AMH-associated Aurignacian blade and bladelet

production, dated by optically stimulated luminescence between 34.0 ± 2.0 ka and 38.4 ± 1.9 ka (Aubry et al., 2020), reveals substantial changes on lithic technology and raw material sources.

The luminescence ages, geological studies of sediments associated with Middle Palaeolithic occupations and lithic refitting have revealed several disconformities and overbank alluvial inundation events in the GFU 5 alluvial record (Dimuccio et al., 2019; Aubry et al., 2020) that could be related with global environmental changes attested in the Greenland ice-core record (Rasmussen et al., 2014; Zilhão, 2021). Even though geoarchaeological record is discontinuous, raw material and technical similarities of lithic assemblages associated with luminescence ages spanning from 80 to 39 ka (Aubry et al., 2020) are strong evidence against environmental forcing, functional or seasonal occupation of the site to explain the similar long-term pattern observed.

Raw material origins and lithic reduction sequences reconstructed from the Middle and Upper Palaeolithic lithic assemblages at the site do not support an interpretation based on differential cognitive, behavioural, and cultural abilities of Neanderthal and AHM. Instead, they highlight distinct land-use strategies associated with Middle and Upper Palaeolithic lithic technology. Even so, we observe a stasis in raw material procurement strategies and no significant reduction of transfer distance or change of lithic raw material origin for the last Middle Palaeolithic occupations (<50 ka), which could be interpreted as a potential proxy of Neanderthal demise. Considering the long chronology of the record, the patterns detected cannot be explained only by environmental forcing. An alternative explanation can be found by using the Forager/Collector's model (Binford, 1980). In a foraging subsistence-settlement system, where hunter-gatherers explore resource patches in day-long round trips around each settlement, before moving to another settlement site when resources are exhausted, it is expected that the raw material discarded on each site should be the result of its immediate geological context. This contrasts with a collector subsistence-settlement system, where hunter-gatherers explore larger areas, directly procuring different resource patches, through group dispersion and aggregation during logistically procurement parties. In this case, discarded raw material should express a larger regional geological context. Therefore, only considering embedded raw material procurement, different subsistence strategies should have different archaeological expressions on the same site. To explain the presence of exotic raw materials, exchange must be added to the equation, requiring larger social networks (Aubry et al., 2012).

The data must be compared with lithic assemblages from regional sites in different geological contexts to confirm if the rarity of quartzite and correlatively the dominance of quartz are characteristics of Middle Palaeolithic in the region. For this, the reduction sequence used through time and the origin of quartzite, quartz and rock crystal of Middle Palaeolithic assemblages must be established more precisely to improve the model inferred from the raw material supply at Cardina-Salto do Boi.

Finally, to disentangle technical and cultural factors in the selection and transportation of regional sources, research must be focused on J1b brown micro-quartz (Fig. 4), which is systematically present during the Upper Palaeolithic in the Côa Valley (Aubry et al., 2012), confirming its use by Neanderthal populations and its diffusion extent.

Acknowledgments

This study is a contribution to the Project PALÆCOA: Neanderthal to Anatomically Modern Human transition in the Côa Valley: Environments, Symbolism and Social networks (PTDC/EPH-ARQ/0326/2014), funded by the Fundação para a Ciência e Tecnologia (FCT) and the Europe 2020 Programme—FEDER (POCI-01-0145-FEDER-016605). The Direção-Geral do Património Cultural provided the permit for this project and the Fundação Côa Parque the logistical support and permission to conduct the project on which this study is based.

Appendix A. Supplementary data

Supplementary data to this article can be found online at https://doi.org/10.1016/j.jasrep.2022.103385.

References

Abrunhosa, A., Marquez, B., Arsuaga, J.L., 2020. O aprovisionamento de matérias-primas líticas no centro da Península Ibérica no Paleolítico Médio: Estado da questão. Arqueol. História 70, 25–38.
Arrizabalaga, A., Altuna, J., 2000. Labeko Koba (País Vasco). Hienas y humanos en los albores del Paleolítico superior. Soc. Ciencias Aranzadi, Munibe 52, 395 p.
Aubry, T., 2009. 200 séculos da história do Vale do Côa: incursões na vida quotidiana do caçadores-artistas do Paleolítico. Trabalhos de Arqueologia 52.
Aubry, T., Almeida, M., Neves, M.J., 2006. The Middle-to-Upper Palaeolithic transition in Portugal: An Aurignacian phase or not? Proceeding of the Symposium "Towards a definition of the Aurignacian", Lisbon, Portugal. In: O. Bar-Yosef and J. Zilhão (eds.). Trabalhos de Arqueologia 45, 95–108.
Aubry, T., Luís, L., Mangado Llach, J., Matias, H., 2012. We will be known by the tracks we leave behind: exotic lithic raw materials, mobility and social networking among the Côa Valley foragers (Portugal). J. Anthropol. Archaeol. 31, 528–550.
Aubry, T., Mangado Llach, X., Matias, H., 2014. Matérias-primas das ferramentas em pedra lascada da Pré-história do Centro e Nordeste de Portugal. In: Dinis, P.A., Gomes, A., Monteiro-Rodrigues, S. (Eds.), Proveniência de materiais geológicos: abordagens sobre o Quaternário. Associação Portuguesa para o Estudo do Quaternário, pp. 165–192.
Aubry, T., Barbosa, A.F., Luìs, L., Santos, A.T., Silvestre, M., 2016a. Quartz use in the absence of flint. Middle and Upper Palaeolithic raw material economy in the Côa Valley (North-eastern Portugal). Quat. Int. 424, 113–129.
Aubry, T., Gameiro, C., Mangado Llach, J., Luís, L., Matias, H., Pereiro, T., 2016b. Upper Palaeolithic lithic raw material sourcing in Central and Northern Portugal as an aid to reconstructing hunter-gatherer societies. J. Lithic Stud. 3 (2) https://doi.org/10.2218/jls.v3i2.1436.
Aubry, T., Dimuccio, L.A., Barbosa, A.F., Luìs, L., Santos, A.T., Silvestre, M., 2020. Timing of the Middle-to-Upper Palaeolithic transition in the Iberian inland (Cardina-Salto do Boi, Côa Valley, Portugal). Quat. Res. 98, 81–101.
Bachellerie, F., 2011. Quelle unité pour le Châtelperronien? Apport de l'analyse taphonomique et techno-économique des industries lithiques de trois gisements aquitains de plein-air: le Basté (Pyrénées-Atlantiques), Bidart (Pyrénées-Atlantiques) et Canaule II (Dordogne). University of Bordeaux I, p. 441. Phd dissertation.
Bar-Yosef, O., 2002. The Upper Palaeolithic revolution. Ann. Rev. Anthropol. 31, 363–393.
Bergadà, M., M. 2009. Análisis micromorfológico de la secuencia sedimentaria de Cardina I (Salto do Boi, Vila Nova de Foz Côa, Portugal), in AUBRY, T. (ed.), 200 séculos de história do Vale do Côa: Incursões na vida quotidiana dos caçadores-artistas do Paleolítico, Lisboa: IGESPAR, I. P., Trabalhos de Arqueologia 52, 112–127.
Binford, L.R., 1980. Willow smoke and dogs' tails: Hunter-gatherer settlement systems and archaeological site formation. Am. Antiq. 45 (1), 4–20.
Boëda, E., 1993. Le débitage Discoïde et le débitage Levallois récurrent centripète. Bull. Soc. Préhistorique Française. Fr. 90 (6), 392–404.
Brantingham, P.J., 2006. Measuring forager mobility. Curr. Anthropol. 47 (3), 435–459.
Burke, A., 2012. Spatial abilities, cognition and the pattern of Neanderthal and modern human dispersals. Quat. Int. 247, 230–235.
Cabral, J., 1989. An example of intraplate neotectonic activity, Vilariça basin, Northeast Portugal. Tectonics 8, 285–303.
Cailleux, A., 1992. Notice sur le Code des Couleurs des sols, Ed. Boubée.
Carvalho, D., 1992. Carta Geológica de Portugal, Escala 1: 500 000. Serviço Geológico de Portugal & Instituto Geográfico e Cadastral, Lisboa.
Cura, S., Grimaldi, S., 2009. The intensive quartzite exploitation in Middle Tagus Valley Pleistocene open air sites – the example of Ribeira da Ponte da Pedra. In: Technological Analysis on Quartzite Exploitation, Proceedings of the XV World Congress UISPP (Lisbon, 4-9 September 2006) (Grimaldi, S. and Cura, S., Eds.), British Archaeological Reports International Series, Vol. 1998, Archaeopress, Oxford, pp. 49–56.
Delagnes, A., Rendu, W., 2011. Shifts in Neandertal mobility, technology and subsistence strategies in western France. J. Archaeol. Sci. 38, 1771–1783.
De la Torre, I., Martínez-Moreno, J., Mora, R. 2013. Change and Stasis in the Iberian Middle Paleolithic. Considerations on the significance of mousterian technological variability. Curr. Anthropol. 54 (8), 320–336.
Delvignes, V., 2016. Géoressources et Expressions Technoculturelles dans le sud du Massif Central au Paléolithique Supérieur: des Déterminismes et des Choix. University of Bordeaux. PhD dissertation.
Demars, P.-Y., 1985. Sur les problèmes de territoires (?) et de circulation des silex (?) Bull. Soc. Linnéenne Lyon, 54 (8), 113–114.
Demars, P.Y., Laurent, P., 1992. Types d'outils lithiques du Paléolithique supérieur en Europe. Cahiers du Quaternaire 14, CNRS édition.
d'Errico, F., 2003. The invisible frontier. A multiple species model for the origin of behavioral modernity. Evol. Anthropol. 12, 188–202.
Deschamps, M., Zilhão, J., 2018. Assessing site formation and assemblage integrity through stone tool refitting at Gruta da Oliveira (Almonda karst system, Torres Novas, Portugal): A Middle Paleolithic case study. PLoS ONE 13 (2), 0192423.
Dibble, H.L., Bar-Yosef, O. 1995. The Definition and Interpretation of Levallois Technology. Prehistory Press.

Dimuccio, L., Aubry, T., Bergadà, M., Rodrigues, N., Cunha, L., 2019. Facies analysis and Late-Pleistocene fluvial depositional environments in the Cardina-Salto do Boi archaeological site (Côa Valley, Portugal). Publicações da Associação Portuguesa de Geomorfólogos 11, 167–170.
Driscoll, K., 2010. Understanding quartz technology in early prehistoric Ireland. Phd dissertation, University College Dublin. 2 vols.
Eren, M.I., Lycett, S.J., 2012. Why levallois? a morphometric comparison of experimental 'preferential' levallois flakes versus debitage flakes. PLoS ONE 7 (1), e29273. https://doi.org/10.1371/journal.pone.0029273.
Féblot-Augustins, J., 1993. Mobility strategies in the Late Middle Palaeolithic of central Europe and western Europe: elements of stability and variability. J. Anthropol. Archaeol. 12, 211–265.
Féblot-Augustins, J., 1999. Raw material transport patterns and settlement systems in the European Lower and Middle Palaeolithic: continuity, change and variability. In: Roebroeks, W., Gamble, C. (Eds.), The Middle Palaeolithic Occupation of Europe. University of Leiden, Leiden, pp. 193–214.
Fernandes, P., Raynal, J.-P., 2006. Pétroarchéologie du silex: un retour aux sources C. R. Palevol 5, 829–837.
Fernandes, P., Raynal, J.-P., Moncel, M.-H., 2008. Middle Palaeolithic raw material gathering territories and human mobility in the southern Massif Central, France: First results from a petro-archaeological study on flint. J. Archaeol. Sci. 35 (8), 2357–2370. https://doi.org/10.1016/j.jas.2008.02.012.
Flügel, E., 2010. Microfacies of Carbonate Rocks. Springer, Berlin, p. 915.
Gamble, C., 1999. The Palaeolithic Societies of Europe. Cambridge University Press, Cambridge.
Geneste, J.M., 1985. Analyse lithique d'industries moustériennes du Périgord: Une approche technologique du comportement des groupes humains au Paléolithique moyen. University of Bordeaux I. PhD Dissertation.
Geneste, J.-M., 1988. Systèmes d'approvisionnement en matières premières au Paléolithique moyen et au Paléolithique supérieur en Aquitaine, in Kozlowski J. (éd.), L'Homme de Néandertal, vol. 8, La Mutation, Liège, ERAUL 35, 61–70.
Gilman, A., 1984. Explaining the upper palaeolithic revolution. In: Springs, E. (Ed.), Marxist Perspectives in Archaeology. Cambridge University Press, Cambridge, pp. 115–126.
Gómez de Soler, B., Marí Soto, M, Vallverdú, J., Vaquero, M., Bargalló, A., Chacón, M.G., Romagnoli, F., Carbonell, E., 2020. Neanderthal lithic procurement and mobility patterns through a multi-level study in the Abric Romaní site (Capellades, Spain) Quat. Sci. Rev. 237. 10.1016/j.quascirev.2020.106315.
Green, R.E., et al., 2010. A draft sequence of the Neandertal genome. Science 328, 710–722.
Haws, J., Benedetti, M.M., Talamo, S., Bicho, N., Cascalheira, J., Ellis, M.G., et al., 2020. The early Aurignacian dispersal of modern humans into westernmost Eurasia. Proc. Natl. Acad. Sci. 117 (41), 25414–25422. https://doi.org/10.1073/pnas.2016062117.
Hoffecker, J.F., 2009. The spread of modern humans in Europe. Proc. Natl. Acad. Sci. 106 (38), 16040–16045.
Hublin, J.-J., 2015. The modern human colonization of western Eurasia: when and where? Quat. Sci. Rev. 118, 194–210.
Hublin, J.-J., et al., 2020. Initial Upper Palaeolithic Homo sapiens from Bacho Kiro cave, Bulgaria. Nature 581, 299–302.
Husson, F., Josse, J., Le, S., Mazet, J. 2018. FactoMineR: Multivariate Exploratory Data Analysis and Data Mining with R. R package version 1.41 [online]. Available: http://CRAN.R-project.org/package=FactoMineR (May 04, 2018).
Higham, T., Jacobi, R., Julien, M., David, F., Basell, L., Wood, R., Davies, W., Ramsey, C. B., 2010. Chronology of the Grotte du Renne (France) and implications for the context of ornaments and human remains within the Châtelperronian. Proc. Natl. Acad. Sci. 107 (47) 20234–20239; 10.1073/pnas.1007963107.
Higham, T., Douka, K., Wood, R., Ramsey, C.B., Brock, F., Basell, L., et al., 2014. The timing and spatiotemporal patterning of Neanderthal disappearance. Nature 512 (7514), 306–309.
Hoffmann, D.L., Angelucci, D.E., Villaverde, V., Zapata, J., Zilhão, J. 2018a. Symbolic use of marine shells and mineral pigments by Iberian Neandertals 115,000 years ago. 2018. Sci. Adv. 4, eaar5255.
Hoffmann, L., Standish, C.D., García-Diez, M., Pettitt, P.B., Milton, J.A., Zilhão, J., et al., 2018b. U-Th dating of carbonate crusts reveals Neandertal origin of Iberian cave art. Science 359 (6378), 912–915.
Hofman, J.L., Enloe, J.G., 1992. Piecing together the past: application of refitting studies in archaeology. BAR International Series 578.
Hublin, J.-J., Talamo, S., Julien, M., David, F., Connet, N., Bodu, P., Vandermeersch, B., Richards, M.-P., 2012. Radiocarbon dates from the Grotte du Renne and Saint-Césaire support a Neandertal origin for the Châtelperronian. Proc. Natl. Acad. Sci. 109, 18743–18748.
Jaubert, J., Verheyden, S., Genty, D., et al., 2016. Early Neanderthal constructions deep in Bruniquel Cave in southwestern France. Nature 534, 111–114. https://doi.org/10.1038/nature18291.
Kelly, R.L., 1983. Hunter-gatherer mobility strategies. J. Anthropol. Res. 39, 277–306.
Klaric, L., Guillermin, P., Aubry, T., 2009. Des armatures variées et des modes de productions variables. Réflexions à partir de quelques exemples issus du Gravettien d'Europe occidentale (France, Portugal, Allemagne). Gallia Préhistoire 51, 113–154.
Klein, R.G., 2003. Whither the Neanderthals? Science 299, 1525–1527.
Langley, M., Clarkson, C., Ulm, S., 2008. Behavioral complexity in Eurasian Neanderthal populations: a chronological examination of the archaeological evidence. Cambridge Archaeol. J. 18, 289–307.
Leroi-Gourhan, A. 1964. Le geste et la parole : Technique et langage. Paris, ed. Albin Michel.
Mangado Llach, J., 2005. La Caracterización y el Aprovisionamiento de los Recursos Abióticos en la Prehistoria de Cataluña: Las Materias Primas Silíceas del Paleolítico Superior Final y el Epipaleolítico, , BAR International SeriesS1420. University of Barcelone, Oxford.
Martí, A.P., Zilhão, J., D'Errico, F., Cantalejo-Duarte, P., Domínguez-Bella, S., Fullola, J. M., Weniger, G.C., Ramos-Muñoz, J., 2021. The symbolic role of the underground world among Middle Paleolithic Neanderthals. Proc. Natl. Acad. Sci. 118(33) e2021495118; 10.1073/pnas.2021495118.
Masson, A., 1981. Pétroarchéologie des Roches Siliceuses, Intérêt en Préhistoire. University of Lyon. PhD Dissertation.
Matias, H., 2016. Raw material sourcing in the Middle Paleolithic site of Gruta da Oliveira (Central Limestone Massif, Estremadura, Portugal). J. Lithic Stud. 3 (2) https://doi.org/10.2218/jls.v3i2.1452.
Mellars, P., 1994. The upper Palaeolithic revolution. In: Cunliffe, B. (Ed.), The Oxford illustrated prehistory of Europe. Oxford University Press, Oxford, pp. 42–78.
Michel, A., 2010. L'Aurignacien récent (post-ancien) dans le Sud-Ouest de la France: variabilité des productions lithiques. Révision taphonomique et techno-économique des sites de Caminade-Est, Abri Pataud, Roc-de-Combe, Le Flageolet I, La Ferrassie et Combemenue. PhD dissertation, Bordeaux I University.
Monteiro-Rodrigues, S., 2011. Pensar o Neolítico Antigo: contributo para o estudo do Norte de Portugal entre o VII e o V Milénios a.C. Centro de Estudos Pré-históricos da Beira Alta, Estudos Pré-Históricos 16.
Mourre V., 2003. Discoïde ou pas Discoïde? Réflexions sur la pertinence des critères techniques définissant le débitage Discoïde, in Peresani M. (Ed.), Discoid Lithic Technology - Advances and implications, Oxford, BAR International Series 1120, 1-18.
Neiva, J.M. 2003. Jazigos portugueses de minérios de urânio e sua génese. In: A Geologia de Engenharia e os Recursos Geologicos, Imprensa da Universidade de Coimbra, 15-76.
Pelegrin, J., 1995. Technologie lithique: le Châtelperronien de Roc-de-Combe (Lot) et de La Côte (Dordogne). Cahiers du Quaternaire 20. Editions CNRS, Paris.
Pelegrin, J., Soressi M., 2007. Le Chatêlperronien et ses rapports avec le Moustérien, in Les Néandertaliens. Biologie et Cultures, B. Vandermeersch, B. Maureille, Eds Éditions du CTHS, Documents préhistoriques 23, 283–29.
Pereira, E., 2001. Carta Geológica de Portugal, escala 1: 200 000 e Noticia Explicativa da Folha 2. Instituto Nacional de Engenharia, Tecnologia e Inovação, Lisboa.
Peresani. M., Fiore. I., Gala, M., Romandini, M., Tagliacozzo, A., 2011. Late Neandertals and the intentional removal of feathers as evidenced from bird bone taphonomy at Fumane Cave 44 ky B.P., Italy. Proc. Natl. Acad. Sci. 108(10): 3888–93.
Pike, W.G.A., Angelucci, D.E., Cooper, M.J., Linscott, B., Matias, H., Zilhão, J., 2016. Reconstructing Neanderthal mobility and range at Gruta da Oliveira, Portugal, using high resolution laser ablation Sr isotope analysis. Proc. Eur. Soc. Study Hum. Evol. 5, 188.
Prieto, A., Yusta, I., García-Rojas, M., Arrizabalaga, A., Baena Preysler, J., 2021. Quartzite procurement in conglomerates and deposits: Geoarchaeological characterization of potential catchment areas in the central part of the Cantabrian Region, Spain. Geoarchaeology 36, 490–510.
R Core Team 2013. R: A language and environment for statistical computing. R Foundation for Statistical Computing, Vienna, Austria [online]. Available: http://www.R-project.org/ (Oct. 29, 2016).
Radovčić, D., Sršen, A.O., Radovčić, J., Frayer, D.W., 2015. Evidence for neandertal jewelry: modified white-tailed eagle Claws at Krapina. PLoS ONE 10 (3), e0119802. https://doi.org/10.1371/journal.pone.0119802.
Rasmussen, O., Bigler, M., Blockley, S.P., Blunier, T., Buchardt, S.L., Clausena, H.B., Cvijanovic, I., et al., 2014. A stratigraphic framework for abrupt climatic changes during the Last Glacial period based on three synchronized Greenland ice-core records: refining and extending the INTIMATE event stratigraphy. Quat. Sci. Rev. 106, 14–28.
Ribeiro, A., 1974. Contribution à Íétude tectonique de Trás-os-Montes oriental. Serviços Geológicos de Portugal (Memórias, Nova Série 24), Lisboa.
Ribeiro, A., 1981. A geotraverse through the Variscan fold belt in Portugal. In: Zwart, H. J., Dornsiepen, U.F. (Eds). The Variscan Orogen in Europe. Geologie en Mijnbouw 60, 41–44.
Ribeiro, M.L., 2001. Carta Geológica Simplificada do Parque Arqueológico do Vale do Côa, escala 1: 80 000. Instituto Geológico e Mineiro, Lisboa.
Ribeiro, A., Antunes, M.T., Ferreira, M.P., Rocha, M.P., Soares, A.F., Zbyszewski, G., Moitinho de Almeida, F., Carvalho, D., Monteiro, J.H., 1979. Introduction à la Géologie Générale du Portugal. Serviço Geológico de Portugal, Lisboa.
Ribeiro, A., Pereira, E., Dias, R., 1990. Allochthonous sequences: structure in the Northwest of the Iberian Peninsula. In: Dallmeyer, R.D., Martinez Garcia, E. (Eds.), Pre-Mesozoic Geology of Iberia. Springer-Verlag, Berlin, pp. 220–236.
Rigaud, J.-P., 1982. Le Paléolithique en Périgord: les données du Sud-Ouest sarladais et leurs implications, 2 vol. Bordeaux I University. Phd dissertation.
Rigaud, J.-P., Simek, J., Delpech, F., Texier, J.P., 2016. The Aurignacian and Gravettian in northern Aquitaine: the contribution of Flageolet I. PALEO 27, 265–295.
Ríos, L., Kivell, T.L., Lalueza-Fox, C., Estalrrich, A., García-Tabernero, A., Huguet, R., et al., 2019. Skeletal anomalies in the neandertal family of El Sidrón (Spain) support a role of inbreeding in neandertal extinction. Sci. Rep. 9, 1697. https://doi.org/10.1038/s41598-019-38571-1.
Rodriguez-Hidalgo, A., Morales; J.I., Cebriá, A., L.A., Courtenay, J.L., Fernández-Marchena, García-Argudo, G., 2019. The châtelperronian Neandertals of Cova Foradada (Calafell, Spain) used Iberian imperial eagle phalanges for symbolic purposes. 10.7287/peerj.preprints.27133.
Romagnoli, F., Bargalló, A., Chacón, M.G., Vaquero, M., 2016. Testing a hypothesis about the importance of the quality of raw material on technological changes at Abric

Romaní (Capellades, Spain): some considerations using a high-resolution techno-economic perspective. J. Lithic Stud. 3 https://doi.org/10.2218/jls.v3i2.1443.
Roussel, M., Soressi, M., Hublin, J.J., 2016. The Châtelperronian conundrum: Blade and bladelet lithic technologies from Quinçay, France. J. Hum. Evol. 95, 13–32.
Sánchez de la Torre, M., Le Bourdonnec, F.X., Gratuze, B., Dubernet, S., Mangado Llach, X., Fullola, J.M., 2017. The geochemical characterization of two long distance chert tracers by ED-XRF and LA-ICP-MS. Implications for Magdalenian human mobility in the Pyrenees (SW Europe). Sci. Technol. Archaeol. Res. 3 (2), 15–27. https://doi.org/10.1080/20548923.2017.1370842.
Shea, J.J., 2011. Homo sapiens is as Homo sapiens was: behavioral variability versus "Behavioral Modernity" in paleolithic archaeology. Curr. Anthropol. 52 (1), 1–35.
Shipton, C., Clarkson, C., Bernal, M.A., Boivin, N., Finlayson, C., Finlayson, G., et al., 2013. Variation in lithic technological strategies among the neanderthals of gibraltar. PLoS ONE 8 (6), e65185. https://doi.org/10.1371/journal.pone.0065185.
Silva, A.F., Ribeiro, M.L., 1991. Carta Geológica de Portugal em escala 1: 50000 e Notícia explicativa da Folha 15-A: Vila Nova de Foz Côa. Serviço Geológico de Portugal, Lisbon.
Silva, A.F., Rebelo, J.A., Ribeiro, M.L., 1989. Carta Geológica de Portugal em escala 1: 50000 e Notícia explicativa da Folha 11-C: Torre de Moncorvo. Serviço Geológico de Portugal, Lisbon.
Straus, L.G., 2020. Neanderthal last stand? thoughts on Iberian refugia in late MIS 3. J. Quat. Sci. https://doi.org/10.1002/jqs.3252.
Soressi, M., Geneste, J.-M. 2011. Special Issue: Reduction Sequence, Chaîne Opératoire, and Other Methods; the Epistemologies of Different Approaches to Lithic Analysis; the History and Efficacy of the Chaîne Opératoire Approach to Lithic Analysis; studying Techniques to Reveal Past Societies in an Evolutionary Perspective. PaleoAnthropology, *2011*, 334–350. 10.4207/PA.2011.ART63.
Talamo, S., Soressi, M., Roussel, M., Richards, M., Hublin, J.J., 2012. A radiocarbon chronology for the complete Middle to Upper Palaeolithic transitional sequence of Les Cottés (France). J. Archaeol. Sci. 39 (1), 175–183.
Tarriño, A., 2001. El sílex en la Cuenca Vasco Cantábrica y Pirineo Navarro: Caracterización y su Aprovechamiento en la Prehistoria. País Vasco/Euskal Herriko Unibertsitatea, University, p. 365. PhD Dissertation.
Terradas, X., 2003. Discoid flaking method: conception and technological variability. In: Discoid Lithic Technology. Advances and Implications M. Peresani (Ed.). BAR International Series 1120.
Thiébault, C., 2013. Discoid debitage stricto sensus: a method adapted to highly mobile Middle Paleolithic groups? Palethnologie (Online). https://doi.org/10.4000/palethnologie.580.
Turq, A., Faivre, J.P., Gravina, B., Bourguignon, L., 2017. Building models of Neanderthal territories from raw material transports in the Aquitaine Basin (southwestern France). Quat. Int. 433, 88–101.
Valladas, H., Mercier, N., Froget, L., Jorons, J.-L., Reyss, J.-L., Aubry, T., 2001. TL dating of Upper Palaeolithic sites in the Coa Valley (Portugal). Quat. Sci. Rev. 20 (5–9), 939–943.
Villa, P., Roebroeks, W., 2014. Neandertal demise: an archaeological analysis of the modern human superiority complex. PLoS ONE 9 (4), e96424. https://doi.org/10.1371/journal.pone.0096424.
Villaverde, V., Real, C., Roman, D., Albert, R.M., Badal, E., Bel, M.A., Bergadà, M.M., et al., 2019. The early Upper Palaeolithic of Cova de les Cendres (Alicante, Spain). Quat. Int. 515, 92–124.
Whallon, R., 2006. Social networks and information: Non "utilitarian" mobility among hunter-gatherers. J. Anthropol. Archaeol. 25, 259–270.
Zilhão, J., 1997. O Paleolítico superior da Estremadura portuguesa. Edições Colibri, Lisboa.
Zilhão, J., 2001. Anatomically archaic, behaviorally modern: the last Neanderthals and their destiny. Stichting Nederlands Museum voor Anthropologie en Praehistoriae, Amsterdam.
Zilhão, J., 2006. Chronostratigraphy of the middle-to-upper paleolithic transition in the Iberian Peninsula. Pyrenae 37, 7–84.
Zilhao, J., 2007. The emergence of ornaments and art: an archaeological perspective on theorigins of "behavioral modernity". J. Archaeol. Res. 15, 1–54.
Zilhão, J., 2021. The late persistence of the Middle Palaeolithic and Neandertals in Iberia: a review of the evidence for and against the "Ebro Frontier" model. Quat. Sci. Rev. https://doi.org/10.1016/j.quascirev.2021.107098.
Zilhão, J., Aubry, T., Carvalho, A.M.F., Zambujo, G., Almeida, F., 1995. O sítio arqueológico paleolítico do Salto do Boi (Cardina, Santa Comba, Vila Nova de Foz Côa). Trabalhos de Antropologia e Etnologia 35 (4), 471–485.
Zilhão, J., Davis, S.J.M., Duarte, C., Soares, A.M.M., Steier, P., Wild, E., 2010. Pego do Diabo (Loures, Portugal): Dating the Emergence of Anatomical Modernity in Westernmost Eurasia. PLoS ONE 5, 8880.
Zilhão, J., Anesin, D., Aubry, T., Badal, E., Cabanes, D., Kehl, M., Klasen, N., et al., 2017. Precise dating of Middle-to-Upper Palaeolithic transition in Murcia (Spain) supports late Neandertal persistence in Iberia. Heliyon 3 (11).
Zilhão, J., Angelucci, D.R., Arnold, L.J., Demuro, M., Hoffmann, D.L., Pike, A.L.G., 2021a. A revised, Last Interglacial chronology for the Middle Palaeolithic sequence of Gruta da Oliveira (Almonda karst system, Torres Novas, Portugal). Quat. Sci. Rev. 258, 106885 https://doi.org/10.1016/j.quascirev.2021.106885.
Zilhão, J., Angelucci, D.E., Arnold, L.J., d'Errico, F., Dayet, L., Demuro, M., et al., 2021b. Revisiting the Middle and Upper Palaeolithic archaeology of Gruta do Caldeirão (Tomar, Portugal). PLoS ONE 16 (10), e0259089. https://doi.org/10.1371/journal.pone.0259089.